CHAPTER 4

RESULTS AND DISCUSSION

CHAPTER 4

4. RESULTS AND DISCUSSION

In this chapter, initially results of feed materials characteristics including both UCH and ICH were discussed. The gasification of feed material was initiated with air as gasifying medium at temperature 700 ℃, which was further increased up to 850 ℃ with a step rise of 50 ℃. During the variation of gasification temperature, the ER was fixed at 0.1. Furthermore, ER was varied from 0.1 to 0.4 keeping gasification temperature fixed for maximum production of H_2 in fuel gas from previous findings. Then after, air as gasifying medium was replaced by humidified air to further increase the H_2 content in produced fuel gas. After successful attempt of humidified air as gasifying medium, gasification was further performed with treated feed material i.e. ICH followed by same gasification medium retrofitted with CO_2. The results of fixed and fluidized bed gasification processes were prepared. The, optimization of process parameters for fluidized bed gasification was performed using RSM.

4. Results and discussion

4.1. Feed characteristics

4.1.1. Compositional analysis

The lignin, cellulose, hemi-cellulose and other extractives present in UCH were found as 47.5, 42.3, 1.1 and 9.1%, respectively with standard error less than 3% by NDF and ADF methods. Since, UCH contains high amount of lignin, it is not suitable for biochemical processes. Results of proximate, ultimate analysis and high heating value

(HHV) of UCH and ICH25 in accordance with ASTM methods are shown in Table 4.1. The UCH contains only 3.4 % of moisture which is very low and 61.3 % of volatile matter by weight. The high amount of lignin, low amount of moisture and enough amount of volatile matter in UCH makes it very much suitable for the gasification. The moisture content of ICH25 was slightly less than UCH because of adsorption of metal constituents from pulp wastewater on to the UCH surface during impregnation, whereas, volatile matter of ICH25 was increased due to organic compounds present in wastewater. The C, H and N during ultimate analysis of UCH were found to be 44.9, 5.5 and 0.9 % by weight, respectively. The S in UCH was below detection limit and O was calculated by difference, which was found to be 48.7 wt%. Furthermore, the chemical formula of UCH was calculated by taking number of mole of nitrogen as unity and found as $C_{53.84}H_{77.80}O_{43.99}N$ (Peavy and Rowe, McGraw Hill Education publication). The amount of C and H content in ICH25 was slightly more than UCH, which may be due to the high total organic carbon present in waste water of pulp and paper industry (Thomson et. al., 2001; Lacorte et al., 2003).

4.1.2. Scanning electron microscopy-energy dispersive X-ray analysis

Scanning electron microscopy-energy dispersive X-ray (SEM-EDX) of UCH and ICH25 were performed at 700 μm magnifications to see the deposition of metal constituents on the surface of ICH25 obtained after impregnation onto the surface of UCH. Images and spectra of SEM-EDX of UCH and ICH25 were shown in Figures 4.1a-b and 4.2a-b. The comparison of elemental composition from SEM-EDX analysis of all samples is shown in Table 4.2. Since EDX, for lighter elements is not so accurate and hence, the standard deviation of values from the EDX analysis can be said up to 10%. There was no any presence of Ca, Fe and Ni but Zn was found to be 0.23 wt% in UCH. The presence of metals (Ca 0.59, Fe 0.21, Ni 0.08 wt %) and increasing the

amount of Zn from 0.23 to 1.42 % were observed in case of ICH25. Moreover, there was an increase in C content from 30.98 in UCH to 54.63 wt% in ICH25 due to the organic compound present in wastewater. The decrease in moisture and increase in C content for ICH25 as compared to UCH was due to the deposition of metals and organic compounds onto the surface of UCH.

Table 4.1 Proximate, ultimate analysis and HHV of UCH and ICH25[a]

	CH	ICH25
Proximate analysis (wt %)		
Moisture content	3.4	3.2
Volatile matter	61.3	62.4
Fixed carbon*	30.1	29.0
Ash	5.2	5.4
Ultimate analysis (wt %)		
C	44.9	45.7
H	5.5	5.8
O*	48.7	47.6
N	0.9	0.8
S	BDL	0.1
HHV (MJ/kg)	23.21	23.41

[a]Standard uncertainties: proximate analysis = 1.5 %; ultimate analysis < 1 %;
BDL- Below detection limit
* by difference

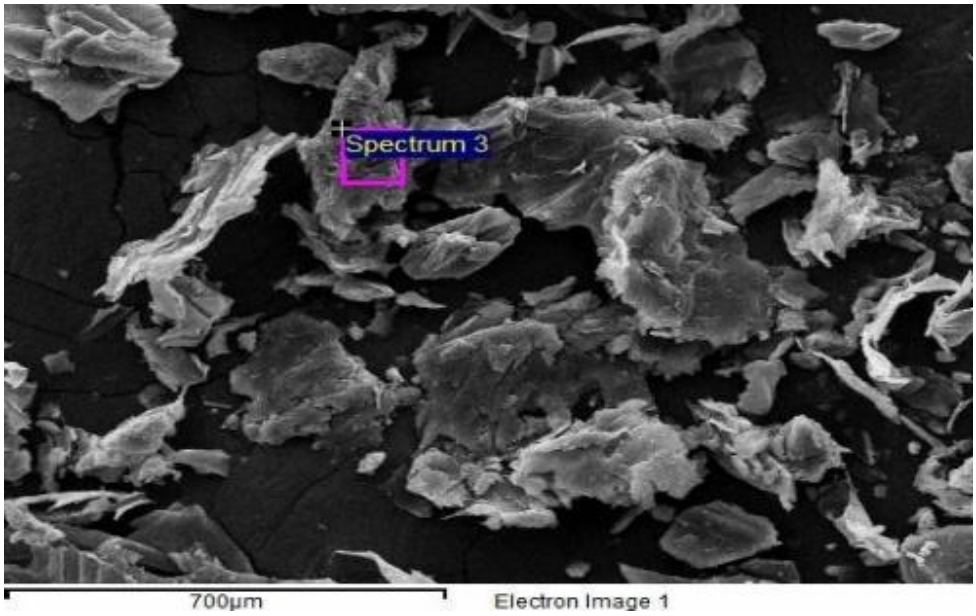

a)

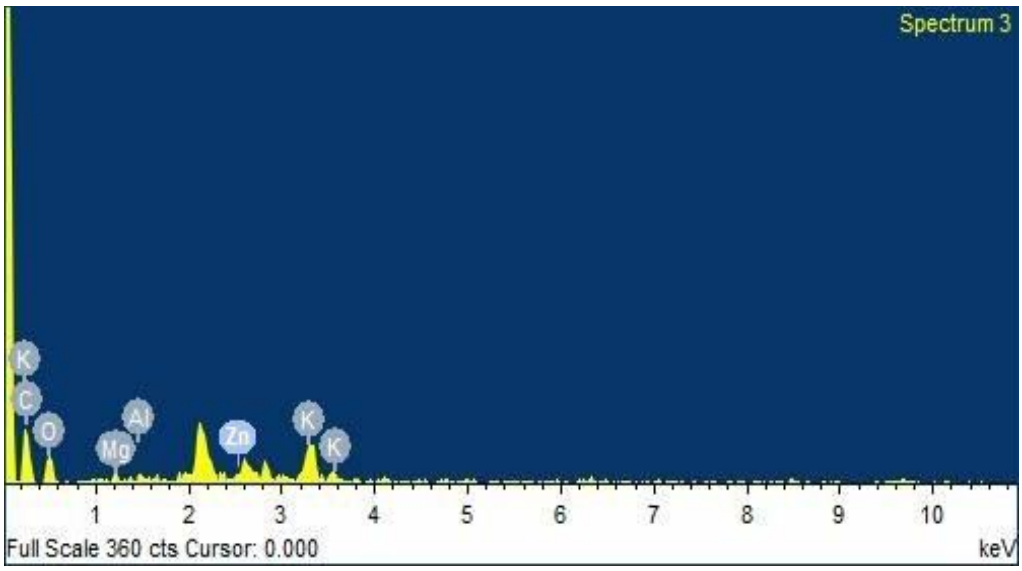

b)

Figure 4.1 a) SEM image and b) EDX spectra of UCH

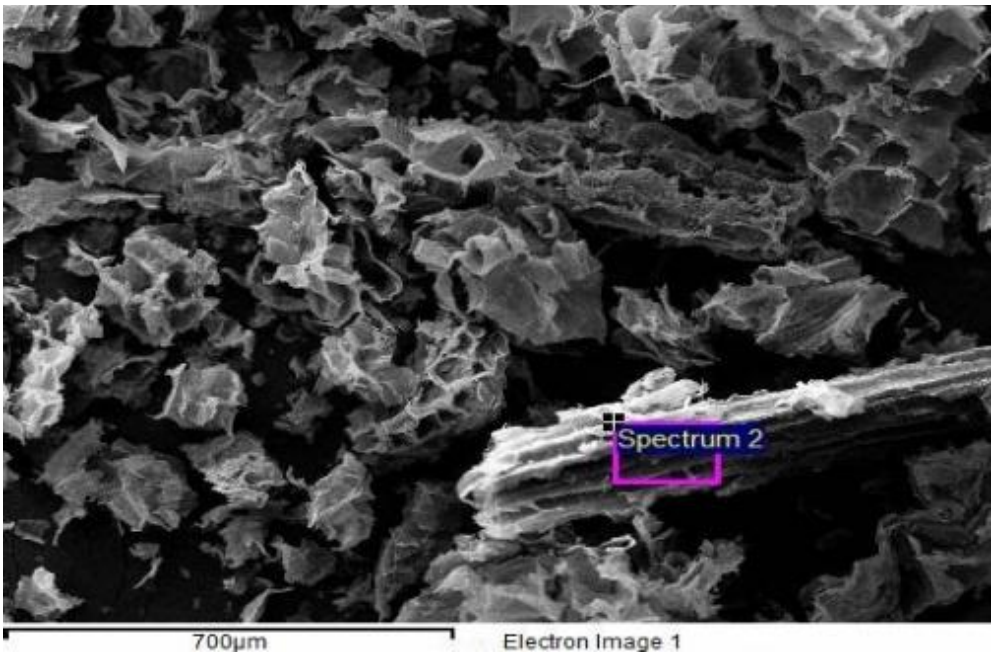

a)

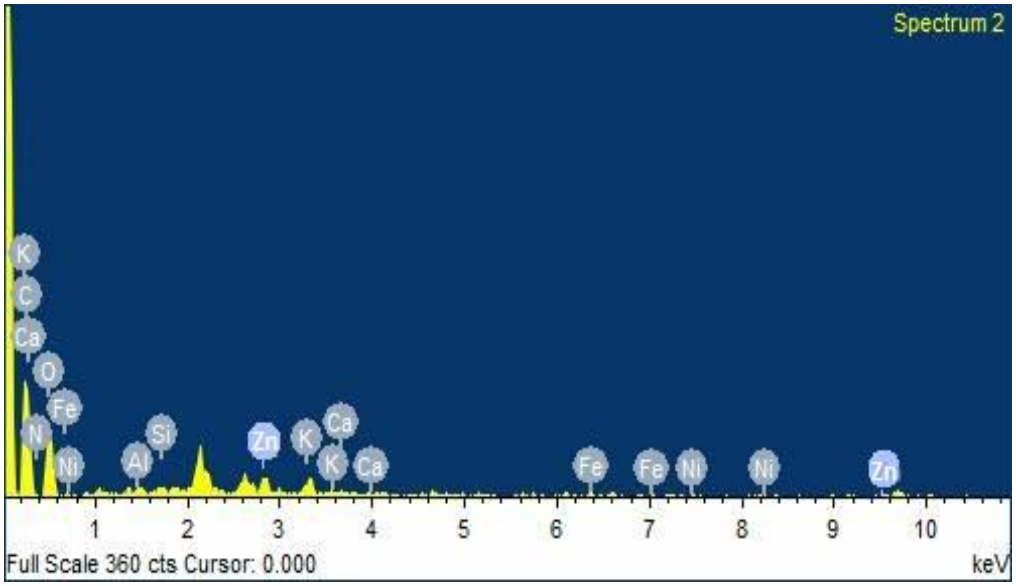

b)

Figure 4.2 a) SEM image and, b) EDX spectra of ICH25

Table 4.2 Comparison of elemental composition of UCH and ICH25

Elements	UCH (wt %)	ICH25 (wt %)
C	30.98	54.63
N	5.61	26.71
O	49.03	9.03
Mg	0.80	0.51
Al	0.72	1.07
Zn	0.23	1.42
Si	-	0.41
K	12.63	5.34
Ca	-	0.59
Fe	-	0.21
Ni	-	0.08

4.1.3. Energy dispersive- X-ray fluorescence analysis

Further, to confirm the deposition of metal constituents on the surface of ICH, the comparative study of Energy dispersive- X-ray fluorescence (ED-XRF) analysis of UCH and ICH105 was performed and the results were shown in Table 4.3. From Table 4.3 it was seen that there was decrease of Ni concentration from UCH to ICH105, however, it showed only 5 and 3 ppm for UCH and ICH105, respectively which might be considered as noise. But there was no any trace of Na in UCH but 8460 ppm of Na was found in ICH105. Furthermore, ICH105 also contained a good amount of increment in elements of CHNO, Si and Ca, which would be beneficial for the catalytic activity to

crack the bond of hydrogen and oxygen of water vapour present with gasifying medium during gasification.

Table 4.3 ED-XRF of UCH and ICH105

Component	UCH (concentration in ppm)	ICH105 (concentration in ppm)
CHNO	940970	942450
Na	-	8460
Mg	4040	2020
Si	4470	4980
P	1593	1405
S	2090	2950
Cl	22000	20210
K	20440	10030
Ca	3150	6860
Ti	35	29
Cr	-	5
Mn	30	22
Fe	465	286
Ni	5	3
Cu	63	37
Zn	38	-
Br	39	10
Rb	89	-
Sr	81	-
Cd	39	25
W	347	191
Pb	21	11
Pt	-	7
Hg	-	3

4.1.4. Fourier-transform infrared spectroscopy of UCH and ICH

Various functional groups have been identified in raw coconut husk and impregnated coconut husk with impregnation temperature 60, 85 and 110 ℃ and changes with respect to untreated coconut husk have been reported. FTIR was studied in wavelength range of 4000 to 500 cm^{-1} in transmittance mode which was varied from approximately 96 to 100 %. ALPHA BRUKER Eco-ATR has been used for the study of FTIR spectra which have been shown in Figure 4.3 and 4.4 for untreated coconut husk and impregnated coconut husk at different temperatures respectively. It could be seen easily that no major changes of functional groups occurs after impregnation of elements from pulp and paper waste water to the surface of UCH. Thus it can be surmised that the change in products after impregnation could be due to metals or other elements like alkali or alkaline but not because of functional group. Furthermore, details of associated functional group with the wavelength have been discussed in more details in other section for fuel oil.

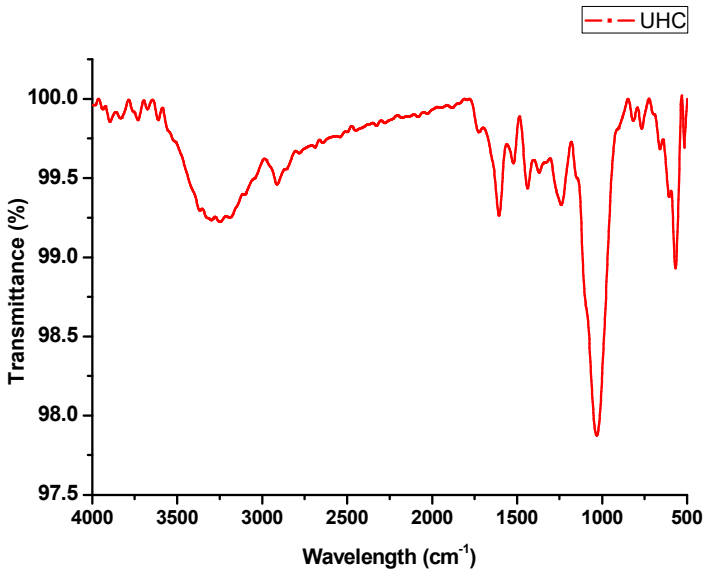

Figure 4.3 FTIR spectra of untreated coconut husk

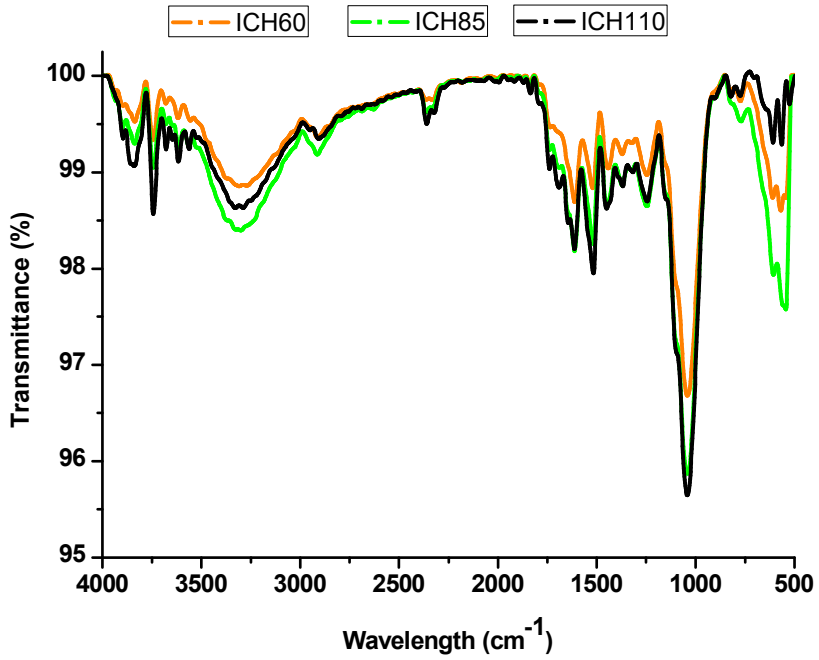

Figure 4.4 FTIR spectra of impregnated coconut husk at temperature 60, 85 and 110 ℃

4.1.5. Thermo gravimetric analysis

Thermo gravimetric analysis (TGA) of the UCH was performed. It is the most efficient instrumental technique to study the thermal behaviour of biomass and other carbonaceous materials. Figure 4.5 illustrated the thermal behaviour of UCH in CO_2 atmosphere at the heating rate of 10℃/min. The descending TG curve signified that weight loss of UCH had occurred with increasing temperature. The thermal disintegration of UCH (lignocellulosic material) revealed the following behaviour which could be described in four different stages. The stage 1 showed the initial weight loss of around 5.6 wt. % between 60 to 140 ℃ due to drying (moisture removal). This was also affirmed by small peak in the DTG curve in the same temperature range. Second stage was the main stage of de-volatilization which started at around 150 ℃ and was almost completed at 420 ℃. There was sharp decrease in TG curve in terms of

weight loss and maximum rate of de-volatilization was observed from DTG curve in this region. This decrease was due to release of volatiles hydrocarbons at high rate from thermal decomposition of hemicellulose, cellulose and some parts of lignin because lignin decomposition occurred at higher temperature (Demiral and Kul, 2014). The weight loss in third stage from 420 to 550 ℃ was mainly because of decomposition of lignin. The fourth and last stage showed slower rate of decomposition of lignin and later at higher temperature no further weight loss was observed. The left over carbon residue after thermal analysis was around 8 wt. %. The above described results from thermal analysis are comparable with results of proximate analysis.

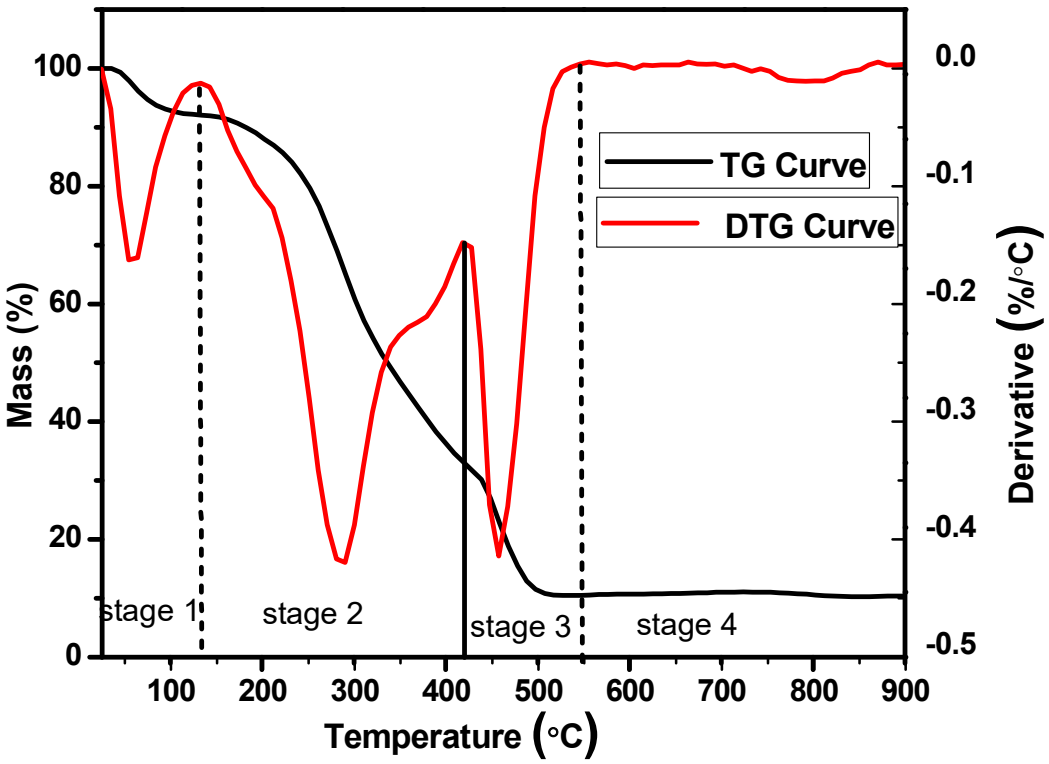

Figure 4.5 Thermo gravimetric analysis of UCH

4.2. Fuel gas composition on fixed bed gasification of UCH

4.2.1. Effect of gasification temperature

As demonstrated by many researchers, the temperature is one of the most important and crucial operating parameters for the performance of biomass gasification process. Thus experiments were performed to study the effects of temperature on fuel gas composition in mole fraction and HHV for UCH by varying temperature from 700 to 850 ℃ with an increment of 50 ℃ at equivalence ratio 0.1 and the results were shown in Figure 4.6. The mole fraction of H_2 produced from UCH was increased from 0.13 to maximum 0.26 on increasing the temperature from 700 to 800 ℃, but diminution was observed on further increasing the temperature above 800 ℃. However, CH_4 was decreased continuously and reached to 0.15 from 0.34 mole fraction by increasing gasification temperature from 700 to 850 ℃. Thus, primary investigation showed the same trend as those obtained by others researchers available in literature (Kopyscinski et al., 2014; Mahapatra et al., 2016; Prasertcharoensuk et. al., 2019; Fiori and Florio, 2010), i.e. higher gasification temperatures favoured more H_2 generation during gasification. When the gasification temperature increased from 700 to 750 ℃, the HHV was decreased from 4.46 to 4.10 MJ/Nm^3. However, it further increased continuously with increase of gasification temperature and reached to highest 4.94 MJ/Nm^3 at gasification temperature 850 ℃.

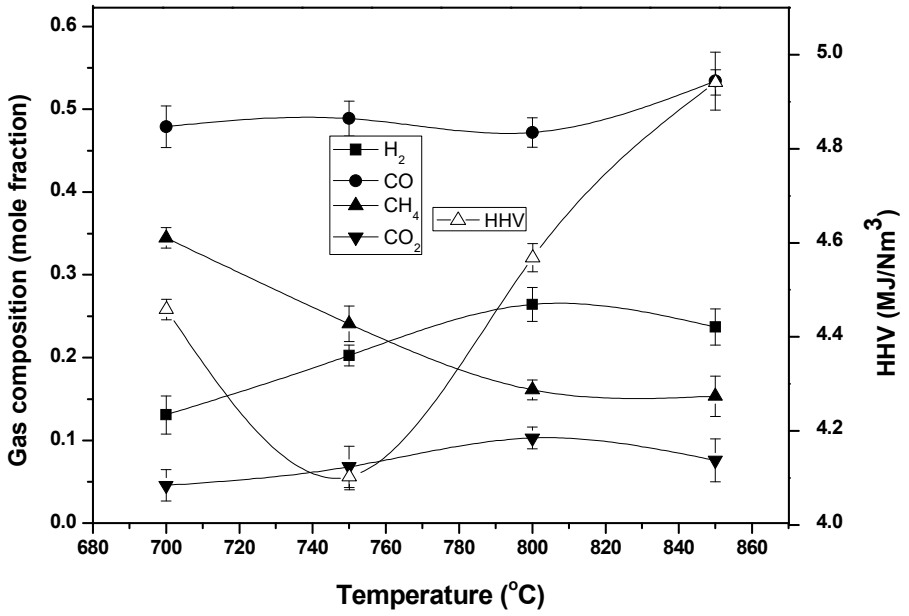

Figure 4.6 Effect of temperature on fuel gas composition and HHV for fixed bed gasification

4.2.2. Effect of equivalence ratio

From the previous study it was found that maximum H_2 production occurred at gasifying temperature of 800 ℃ for the gasification of UCH at equivalence ratio 0.1. Equivalence ratio (ER) is the ratio of actual amount of oxygen supplied to the gasification chamber to the oxygen required stoichiometrically for complete combustion. Since, gasification occurs at limited oxygen, thus ER is another important process parameter that need to be optimised. During current study of gasification of UCH, the ER was varied from 0.1 to 0.4 by keeping gasification temperature fixed at 800 ℃ and the results were shown in Figure 4.7. Increasing ER continuously decreased H_2 which reached to 0.11 mole fraction at ER 0.4 from 0.26 at ER 0.1. However, CO_2 mole fraction increased continuously with the increase of ER. Mole fraction of CO_2 was

only 0.10 at ER 0.1 which reached to 0.28 at ER 0.4. This trend was observed because increase of ER provides more oxygen to gasifying chamber which leads to combustion rather than gasification. Afain the increase in flow rate of air from 0.8 L/min for ER 0.1 to 3 L/min for ER 0.4 lowers the residence time of the evolved gases including gasifying medium for reformation. The mole fraction of CO increased during ER 0.1 to 0.3, and then it got decreased on further increasing the ER. The HHV was found to be highest 5.3 MJ/Nm^3 at ER 0.3. It was because of the high concentration of CH_4 at ER 0.3, which has HHV approximately three times of H_2 per mole basis.

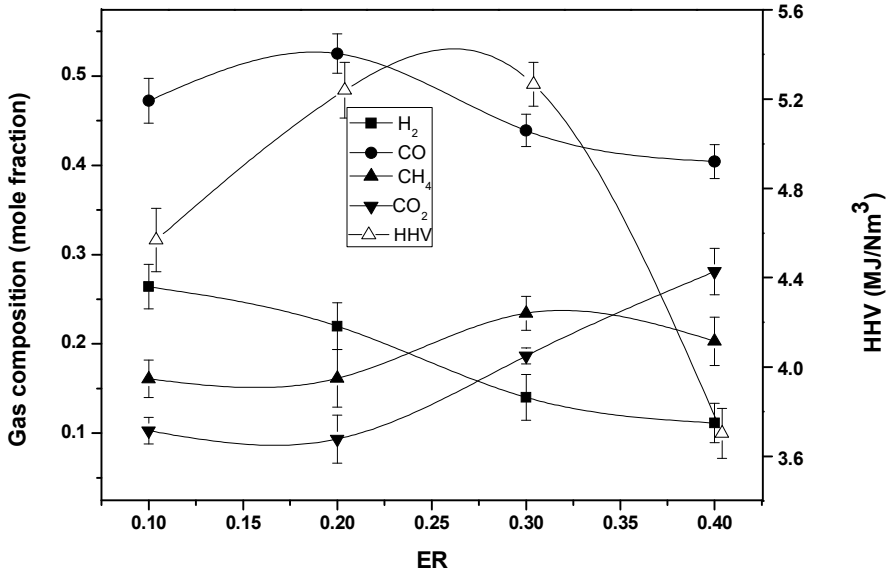

Figure 4.7 Effect of equivalence ratio on fuel gas composition for fixed bed gasification

4.2.3. Effect of relative humidity

The presence of water vapour in the gasifying medium is helpful to improve the quality of fuel gas with regard to H_2 content in biomass gasification. The saturated amount of water vapour present in air is highly dependent on the air temperature. In the present

study, the humidified air temperature was kept approximately at 50 ℃, and relative humidity (RH) was varied from 55 to 95 % with accuracy ±1%. The water vapour to dry air ratio at saturation for air temperature 50 ℃ is 0.087 kg H_2O/kg dry air (Engineering tool box, online). The effect of humidified air on fuel gas composition and HHV at gasification temperature 800 ℃, average particle size 0.72 mm and ER 0.1 was analyzed and depicted in Figure 4.8. Initially at lower RH, the mole fraction of H_2 was found as 0.19, which was further increased to 0.22 mole fraction at RH 95%. In addition, with the increase of RH all components of fuel gas were increased. As moving from RH 55 to RH 95 %, CH_4 was increased from 0.23 mole fractions to 0.29. Furthermore, HHV of fuel gas was highest at RH 95 % which was 8.81MJ/Nm^3. The high concentration of hydrogen in fuel gas was resulted due to the fact that the water vapours may act as strong oxidizing agent beyond the gasification temperature of 600 °C (Feng et al., 2004). Similar type of results in regard to hydrogen yield using steam as gasifying medium was also reported in literature. Nipattummakul et. al. (2012) found maximum of 67% (approx.) hydrogen content by volume via steam gasification of oil palm trunk. Furthermore, they also reported the decrease in hydrogen content to 62% (approx.) with increase of steam flow rate from 4.12 to 7.75 gm/min. Also, 56.09 vol% of hydrogen generation was reported for steam gasification of sewage sludge at temperature 900 and 1000 °C by Nipattummakul et. al. (2010).

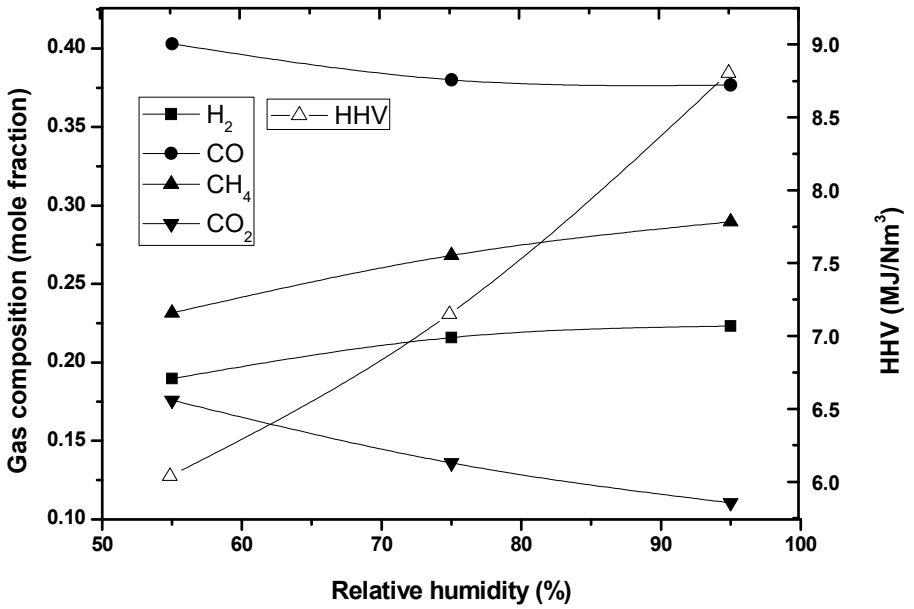

Figure 4.8 Effect of relative humidity on fuel gas composition and HHV for fixed bed gasification

4.2.4. Effect of feed particle size

Since, highest production of H_2 occurred at RH 95 %. Thus, fuel gas composition and HHV were analysed by varying the particle size of UCH at a gasification temperature of 800 °C, RH 95 % and ER 0.1 and it was shown in Figure 4.9. The average particle size of UCH was varied from 0.2 to 3.0 mm. It was depicted from Figure 4.9 that initially the mole fraction of all the components was shown similar to composition with particle size. However, a close examination revealed that H_2 production was highest for particle size 0.25 mm of UCH and after that it showed minor decrease with increase in the particle size up to 3 mm. It could be inferred that the lower particle size (0.25 mm) showed improved mole fraction of the H_2 due to higher surface area incurred. This may be due to fact that for small particle size (0.25 mm), the gasification of biomass is

reaction kinetics controlled and for increasing particle size from 0.75 to 3 mm the resultant product gas trapped inside the particle is more difficult to diffuse out, and the process may be controlled by gas diffusion (Lv et al., 2004). Approximately variation of 0.4 MJ/Nm^3 was found for HHV during gasification for particle size ranging from 0.2 to 3 mm.

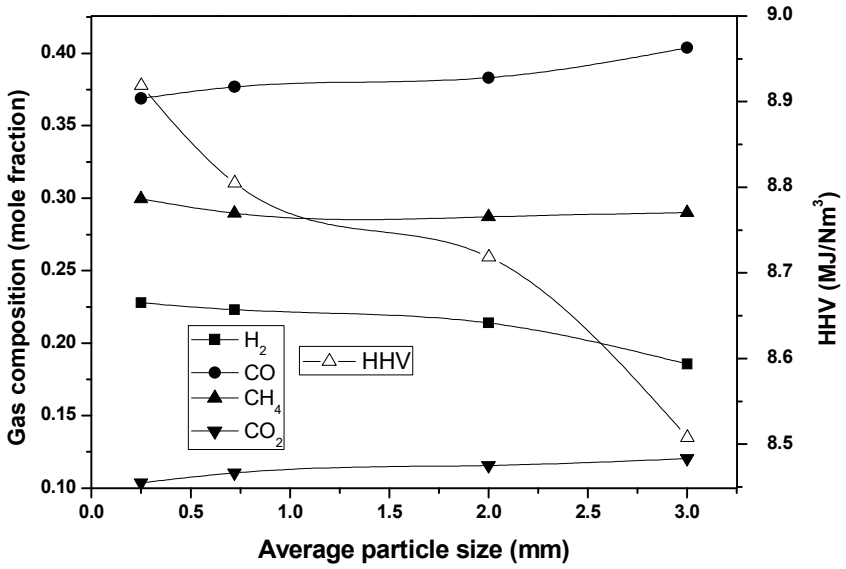

Figure 4.9 Effect of particle size on fuel gas composition and HHV for fixed bed gasification

4.2.5. Effect of gasification temperature with humidified air

Since, there was no major effect of particle size, and hence the UCH with average size of 0.72 mm was shown in large amount for all composition with respect to other sizes. Thus analysis was continued with the UCH particle size of 0.72 mm. As per the previous findings the presence of water vapour in the gasifying medium improved the fuel gas quality in terms of hydrogen content. During this analysis effect of temperature

on the fuel gas composition and HHV were studied. The temperature was varied from 750 to 850 ℃ keeping RH and ER fixed at 95 % and 0.1 and the results on produced gas composition and HHV were shown in Figure 4.10. It was observed from Figure 4.10 that there was a steep rise in mole fraction of H_2 from 0.11 to 0.30 on increasing temperature from 700 to 850 ºC and HHV of fuel gas was also increased from 5.56 to 9.94 MJ/Nm^3 for UCH. Since water gas shift reaction is exothermic (equation (1.4)), hence it is less favourable at a higher temperature. Thus, it could be surmised that the increase in H_2 mole fraction for UCH was due to methane steam reforming and tar steam reforming as depicted in (equations (1.5), (1.6) and (4.1)). This is in agreement with the results of Aranda et al. (2016) and, Li and Suzuki (2009) that steam gasification in the presence of steam fosters the H_2 and decreases CO, CH_4, C_2H_4 and C_2H_6 contents in the fuel gas. It could also be concluded that several important reactions like water gas shift reaction, methane reforming reaction, etc. occur during gasification process. Thus it decreases the concentration of CH_4 from 0.40 to 0.23 mole fraction.

Water gas shift reaction:

$$CO + H_2O \rightarrow CO_2 + H_2 \qquad \Delta H = -41.98 \text{ kJ} \tag{1.4}$$

CH_4 steam reforming:

$$CH_4 + H_2O \rightarrow CO + 3H_2 \qquad \Delta H = +206 \text{ kJ} \tag{1.5}$$

Tar steam reforming reaction:

$$\text{Tar} + H_2O(g) \rightarrow CO + CH_4 + H_2 + C_nH_m \tag{1.6}$$

Tar steam reforming reaction can also be written as

$$C_nH_mO_p + (2n-1)\, H_2O \rightarrow nCO_2 + (1/2m + 2n-p)\, H_2 \tag{4.1}$$

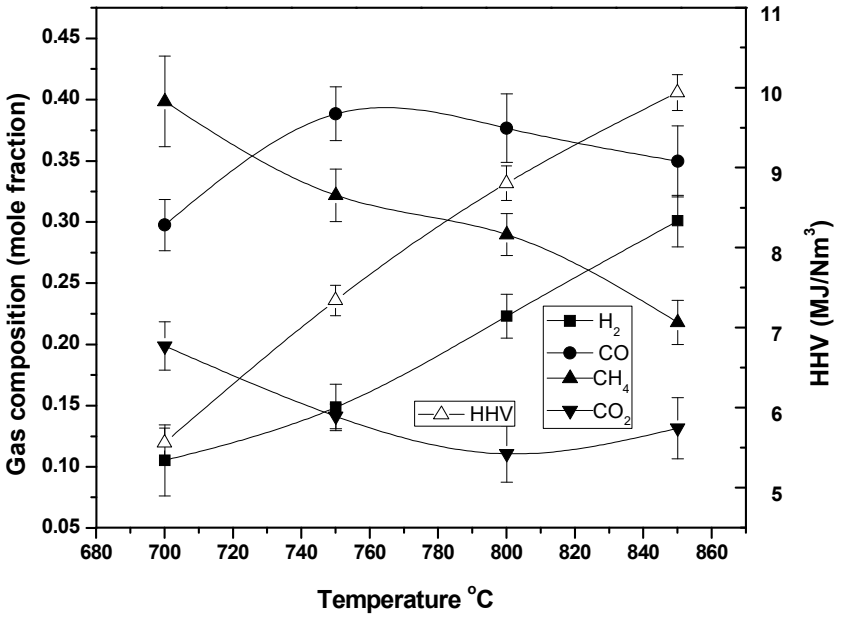

Figure 4.10 Effect of temperature on fuel gas composition at HER 0.1 for fixed bed gasification

4.2.6. Effect of equivalence ratio with humidified air

In this analysis, gasification of UCH was carried out with varying equivalence ratio from 0.1 to 0.4 at gasification temperature of 850 ℃ and inlet air humidity 95 % maintained at 50 ℃. The humidified air at those specific equivalence ratios was named as humidified air equivalence ratio (HER). The fuel gas composition and HHV of fuel gas were shown in Figure 4.11. It was observed that the H_2 mole fraction decreased continuously and reached from 0.25 mole fraction to 0.22 with increase of HER from 0.1 to 0.4, however, CO_2 increased after HER 0.2. The mole fraction of CO was also increased with increase of HER from 0.1 to 0.2, but it followed decreasing trends above HER 0.2. Furthermore, when compared with air as gasifying medium as shown in Figure 4.7, there were similarities in decreasing of H_2 and increasing of CO_2 but mole

fraction of H_2 was more during humidified air gasification. The decrease of H_2 and increase of CO_2 mole fraction were due to the partial combustion in presence of O_2 at high temperature. Moreover, due to steam reforming, H_2 mole fraction was more with respect to air gasification. However, the generation of H_2 may be enhanced in the presence of some catalyst. The value of HHV was also decreased with increase of HER and reached to 4.64 MJ/Nm^3 at HER 0.4 from 9.94 MJ/Nm^3 at HER 0.1.

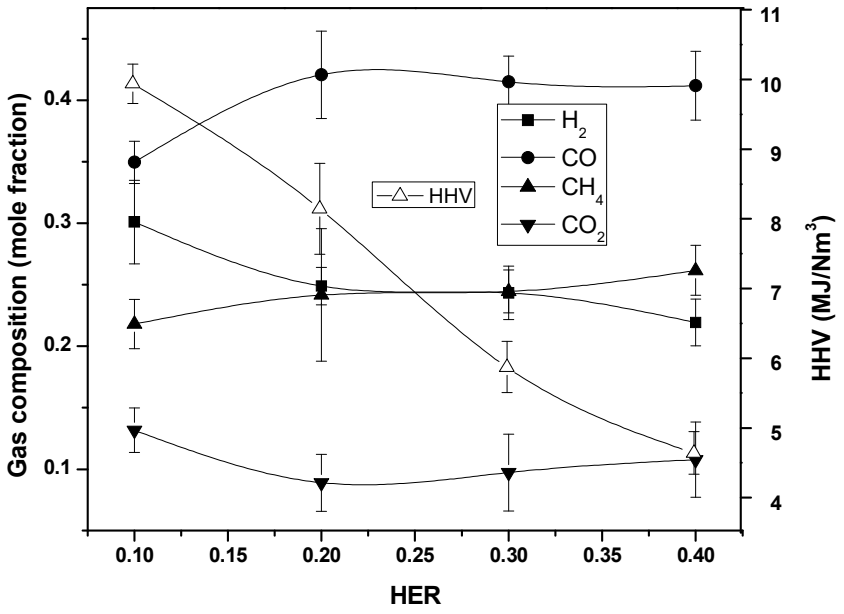

Figure 4.11 Effect of equivalence ratio on fuel gas composition and HHV with humidified air

4.2.7. Effect of CO_2 addition

From Figure 4.7 and Figure 4.11, it was inferred that humidified air as gasifying medium increased the mole fraction of H_2 but decreased the mole fraction of CO. But the mole fraction of both the constituents are important for the conversion of gaseous fuels into liquid fuel via Fischer-Tropsch synthesis and, di-methyl ether (DME) which are shown in Equations 4.2(a), 4.2(b) and 4.3(a), 4.3(b), respectively. Owing to this, CO_2 was added with air and humidified air as gasifying media and the results were analysed.

$$nCO + (2n+1)H_2 \rightarrow C_nH_{2n+2} + nH_2O \quad \text{4.2(a)}$$

$$nCO + (2n)H_2 \rightarrow C_nH_{2n} + nH_2O \quad \text{4.2(b)}$$

$$3H_2 + 3CO \rightarrow CH_3OCH_3 + CO_2 \quad \text{4.3(a)}$$

$$4H_2 + 2CO \rightarrow CH_3OCH_3 + H_2O \quad \text{4.3(b)}$$

Thus, to increase the CO mole fraction in fuel gas composition CO_2 was added with gasifying medium air and humidified air during the gasification of UCH. During this investigation 50% pure CO_2 balanced with N_2 was mixed with air and humidified air at CO_2 flow rate 900 cm^3/min per kg of biomass. Flow rate of air and humidified air were set as per requirement to maintain ER and HER 0.1. Effect of CO_2 addition onto the composition and HHV of fuel gas was shown in Figure 4.12. H_2 concentration was 0.09 mole fraction with air and 0.18 mole fractions with humidified air. Furthermore, CO concentration with air was 0.47 mole fraction whereas, with humidified air it was diminished to 0.36 mole fraction. HHV of the fuel gas produced with air was 5.95 MJ/Nm^3 which reached to 9.04 MJ/Nm^3. CH_4 concentrations was also increased from 0.08 to 0.22 mole fraction when humidified air was used instead of air as gasifying

medium. CO_2 concentration was decreased from 0.34 mole fraction to 0.24. It can be inferred from the result that, increase of mole fraction of CO and decrease of CO_2 concentration was due to Boudouard reaction (Li et al., 2009(a)) as shown in Equation (4.4).

$$C + CO_2 \rightarrow 2CO \qquad \Delta H = +172\ kJ/mol \tag{4.4}$$

Although, humidified air gasification produced good concentration of H_2 and decreased the concentration of CO, but the concentration of CH_4 was also in high amount which is considered as a greenhouse gas. So, the concentration of CH_4 needs to be reduced.

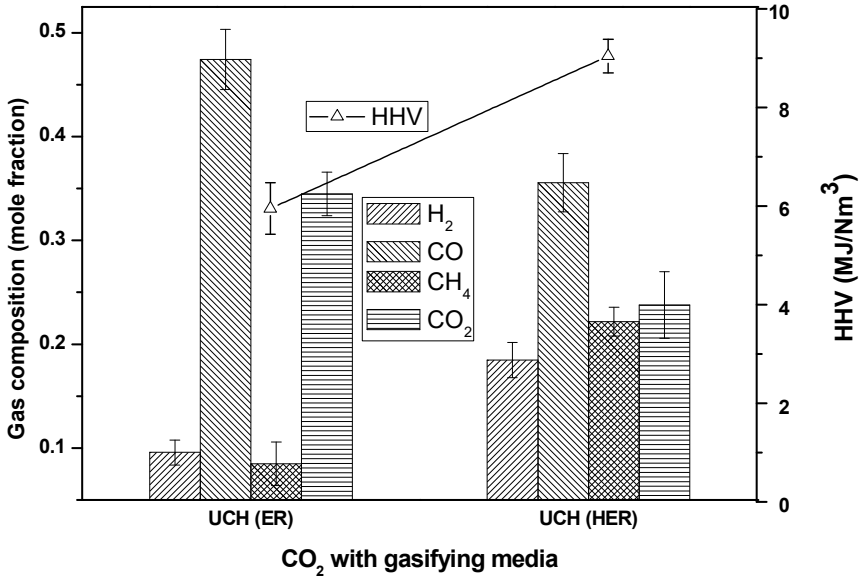

Figure 4.12 Effect of CO_2 addition on fuel gas composition and HHV for fixed bed gasification

4.3. Fuel gas composition on fixed bed gasification of ICH

After gasification of UCH with air, humidified air and addition of CO_2 in it as gasifying medium, further gasification of ICH25 were performed with air and humidified air

retrofitted with CO_2. Furthermore, at optimum conditions of operating parameters, experiments were extended for ICH65 and ICH105 and gasifier performance was analysed.

4.3.1. Effect of gasification temperature with air

In this section gasification of ICH25 was carried out by varying gasification temperature from 700 to 850 ℃, with increment of 50 ℃. AT temperature 700 ℃ the mole fraction of H_2 was same as for both UCH (Figure 4.6) and ICH25 (Figure 4.13), but increasing gasification temperature produced more mole fraction of H_2 than UCH and reached maximum to 0.37 mole fraction at 850 ℃. Mole fraction of CO decreased continuously with increase of gasification temperature and reached from 0.49 mole fraction at 700 ℃ to 0.37 mole fraction at 850 ℃. Furthermore, CH_4 and CO_2 were also decreased with increase of gasification temperature. However, HHV in terms of MJ/Nm^3 decreased with temperature because of the decrease of CH_4. It could be inferred that sharp increase in the mole fraction of H_2 with decrease of CH_4 were due to catalytic activity of the metals deposited onto the UCH surface and because of total organic carbon (TOC) present in the pulp and paper waste water.

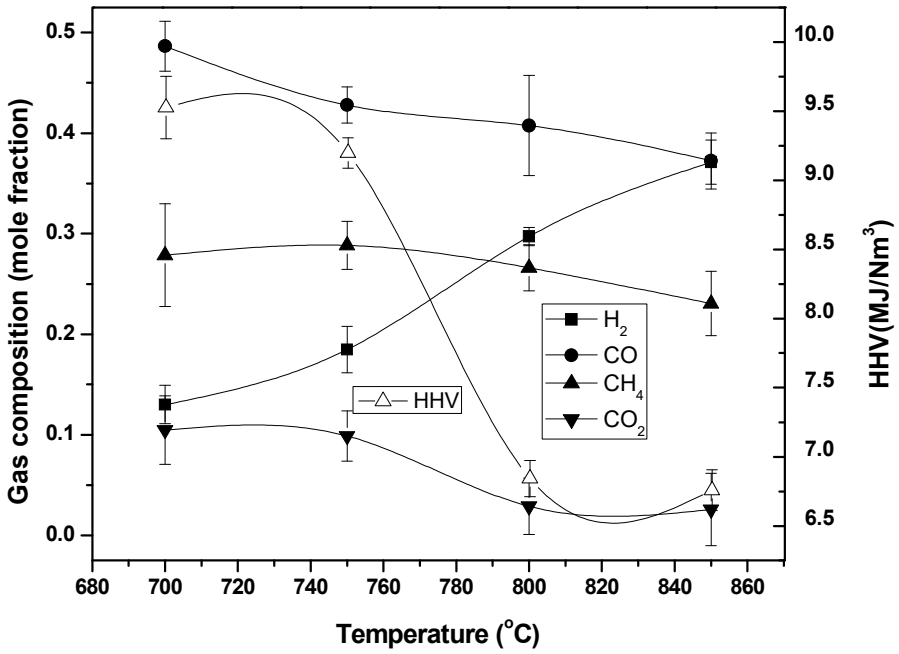

Figure 4.13 Effect of temperature on fuel gas composition and HHV (ICH) for fixed bed gasification

4.3.2. Effect of equivalence ratio

From the previous study it was found that for the gasification of ICH25, the highest mole fraction was yielded at 850 ℃. But to compare it with UCH, the further analysis were performed by varying ER 0.1 to 0.4 at temperature 800 ℃ and shown in Figure 4.14. The trends of the mole fractions of each component followed more or less the same pattern as of UCH. Increasing the ER generates more CO and CO_2 because of more volume of oxygen present in the gasifying medium which leads to partial combustion of ICH25. However, H_2 increased from 0.30 mole fraction to 0.38 with increase of ER from 0.1 to 0.2. Moreover, it decreased continuously with further increase of ER and, HHV also decreased from 6.8 MJ/Nm^3 at ER 0.1 to 4.4MJ/Nm^3 at

ER 0.4. It was because of the decrease of both H_2 and CH_4. So, it can be surmised that higher ER is not favourable for gasification of UCH or ICH25.

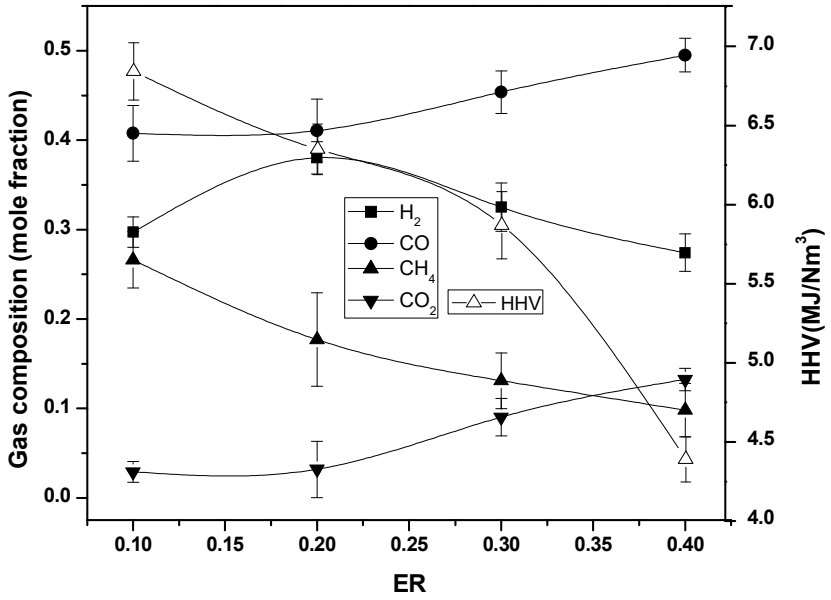

Figure 4.14 Effect of temperature on fuel gas composition and HHV for fixed bed gasification

4.3.3. Effect of gasification temperature with humidified air

In this study gasification of ICH25 was performed with humidified air as gasifying medium at ER 0.1 and gasification temperature varying from 700 to 850 ℃. Humidity of inlet air was 95% with accuracy ±1% for inlet air temperature 50 ℃. Initially at lower temperature 700 ℃, CH_4 was at highest (0.44) and H_2 was at lowest (0.21) mole fraction as shown in Figure 4.15. Increasing the gasification temperature increased the mole fraction of H_2 which reached to maximum 0.54 mole fraction at gasification temperature 850 ℃. Moreover, increasing the gasification temperature from 700 to 850 ℃ decreased the mole fraction of CH_4 from 0.44 to 0.22 respectively. Since water gas

shift reaction is exothermic (equation 1.4), hence it was less favourable at a higher temperature. Thus, it was attributed that the increase in H_2 mole fraction for ICH25 was due to methane steam reforming and tar steam reforming as depicted in equations (1.5) and (1.6) which was engendered because of presence of metals as shown in Table 4.2. These metals showed catalytic property, which increased the rate of the reactions which brisked the generation of H_2 and thus, mole fraction of H_2 was more in ICH25 than UCH. Furthermore, mole fraction of CO was found maximum at gasification temperature 800 ℃, whereas, CO_2 mole fraction was almost same between 0.01 to 0.02 mole fraction at and above 750 ℃. HHV was also found highest 9.5 MJ/Nm^3 at gasification temperature 800 ℃. At this gasification temperature the mole fraction of H_2, CO, CO_2 were 0.37, 0.32, and 0.29 respectively.

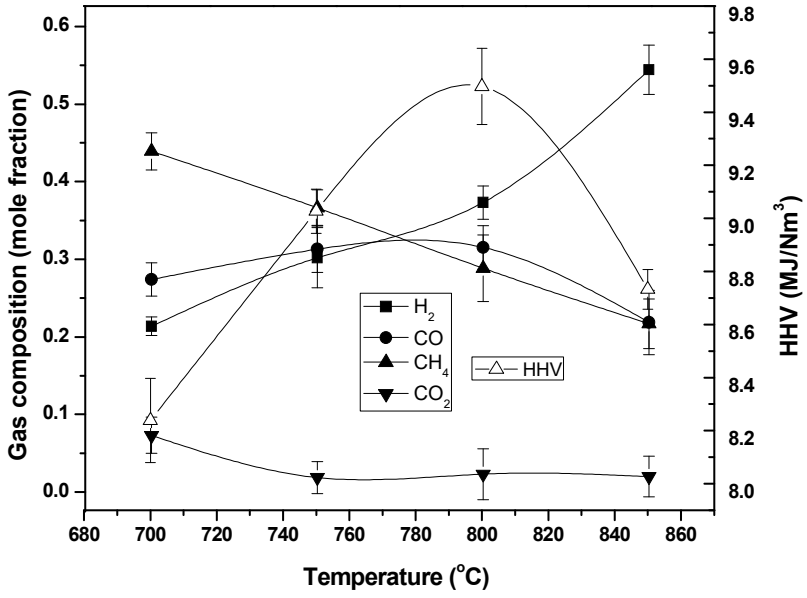

Figure 4.15 Effect of gasification temperature on fuel gas composition for fixed bed gasification

4.3.4. Effect of humidified air equivalence ratio

Gasification of ICH25 was performed at gasification temperature corresponding to highest mole fraction of H_2 with humidified air. Keeping the gasification temperature fixed HER was varied as before from 0.1 to 0.4 and it was shown in Figure 4.16. It could be seen from the Figure 4.16 that although H_2 mole fraction was more in ICH25 than UCH with humidified air, but increasing the HER decreased the H_2 mole fraction. And, it was reached from 0.54 mole fraction at HER 0.1 to 0.29 at HER 0.4. Moreover, increasing HER also decreased the mole fraction of CH_4 and reached to 0.10 from 0.22. However, CO_2 was also increased along with CO for increasing HER, which was unsought component in the fuel gas composition. Thus, it was surmised that presence of water vapour in gasifying medium increased the H_2 mole fraction in fuel gas. Furthermore, impregnations of metal constituents from pulp and paper industry waste water brisked the H_2 formation due to catalytic activity. Moreover, either increases of ER or HER decreased the H_2 mole fraction and it led to partial combustion.

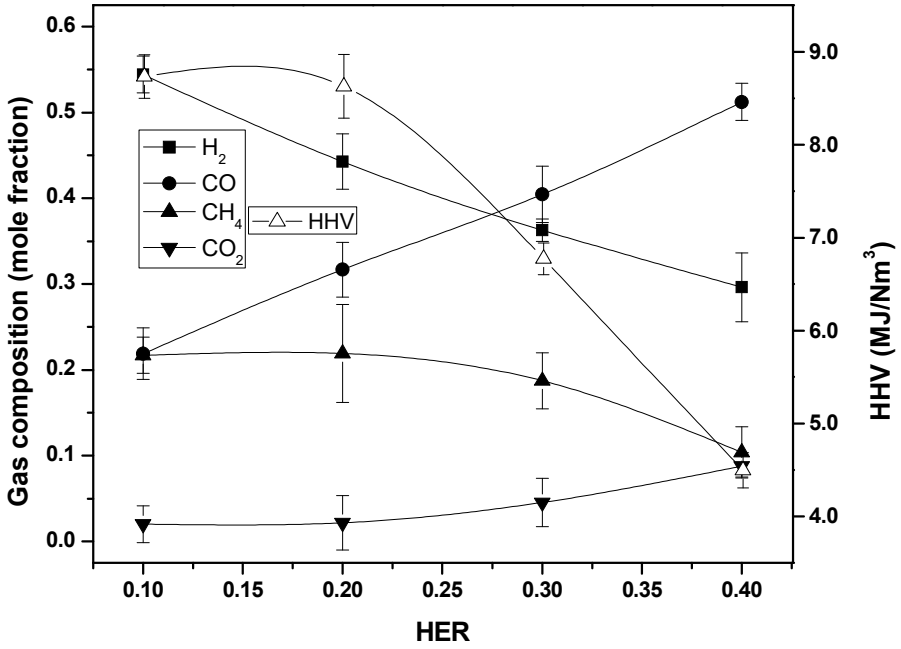

Figure 4.16 Effect of HER on fuel gas composition and HHV for fixed bed gasification

4.3.5. Effect of impregnation temperature

Till now the discussion was limited to coconut husk impregnated only at 25 ℃. Further impregnations were performed at two more temperatures (65 and 105 ℃) and comparative studies were made between UCH, ICH25, ICH65 and ICH105 at optimum operating conditions. The optimum gasifying temperature for air as gasifying medium was 800 ℃ whereas, for humidified air the optimum gasifying temperature was 850 ℃. The equivalence ratio for the both gasifying medium was 0.1. Thus, effect of impregnation temperatures at ER and HER 0.1 on gasification were shown in Figure 4.17a and 4.17b, respectively. H_2 content was increased from mole fraction of 0.26 to 0.40 at ER 0.1. Further with increasing impregnation temperature from 25 to 105 ℃ the mole fraction of H_2 was increased from 0.30 to 0.61 at HER 0.1. It can be inferred that

higher impregnation temperature was more favourable for H_2 production. ED-XRF result in Table 4.3 also showed deposition of Na, Si and Ca onto ICH at impregnation temperature 105 °C. It could also be surmised from a higher mole fraction of H_2 in humidified air gasification that the cracking of H_2O molecules was more brisked with the catalytic activity due to impregnation onto UCH. The similar trends were also found by Wang et al. (Wang et al., 2016) using Zn and Zhang et al. (Zang et al., 2015) using Ni as catalyst. Further, the CH_4 content was maximum 0.29 mole fraction on air gasification at impregnation temperature 65 °C. Whereas, in humidified air gasification CH_4 was lowest at highest impregnation temperature 105 °C. It could be engendered that the cracking of H_2O molecules also produced oxygen which led to the oxidation process due to which the CO_2 content was also increased from 0.01 to 0.08 mole fraction from ICH25 to ICH105.

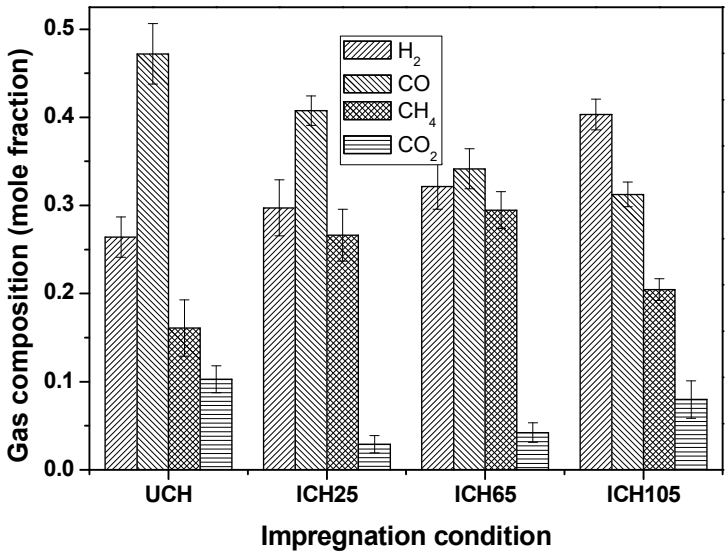

a)

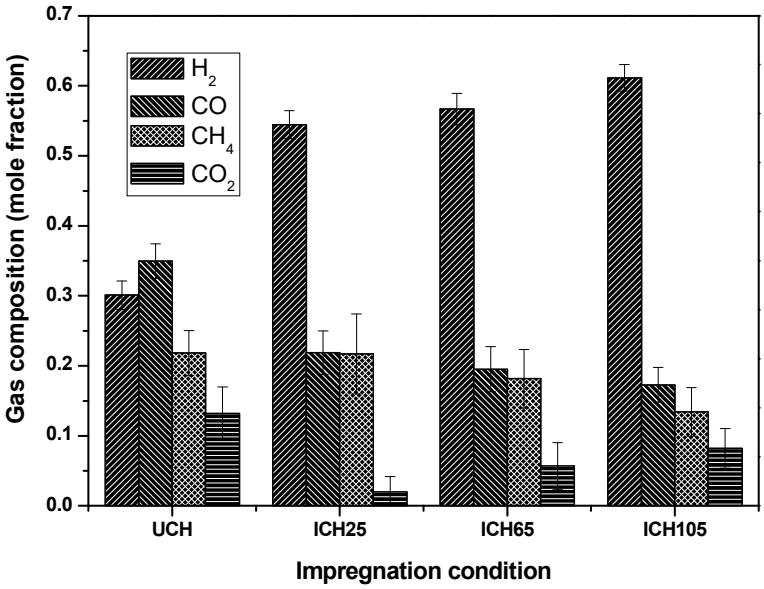

b)

Figure 4.17 Gas composition and HHV a) at fixed bed gasification temperature 800 ℃ with ER 0.1, and b) at fixed bed gasification temperature 850 ℃ with HER 0.1

4.3.6. Effect of CO_2 addition in gasifying media

From the previous study it was found that, there were substantial difference in the mole fraction of H_2 and CO in the fuel gases produced from ICH25, ICH65, and ICH105. So, an effort was made by adding CO_2 with gasifying media to make the composition of CO comparable with H_2 without decreasing the amount of H_2 and HHV. Thus, the effect of CO_2 addition on gas composition and HHV was investigated for ICH25 and ICH105 with both the gasifying media air and humidified air at ER and HER 0.1 and the results were shown in Figure 4.18. The CO_2 was 50% pure, and flow rate was kept at 900 cm^3/min per kg of biomass along with air or humidified air as per requirement. There

were increasing trends of H_2 from air to humidified air for both ICH25 and ICH105. The highest mole fraction of H_2 0.40 mole fraction was yielded for ICH105 with humidified air as compared to air which was 0.29 mole fraction. Furthermore, CO was also in appreciable amount 0.29 mole fraction. It was due to the fact that Boudouard reaction was more favourable in ICH105 than ICH25 as expressed in Equation 4.3. The HHV was also found maximum 12.6 MJ/Nm^3 for TCH105 among all the processes.

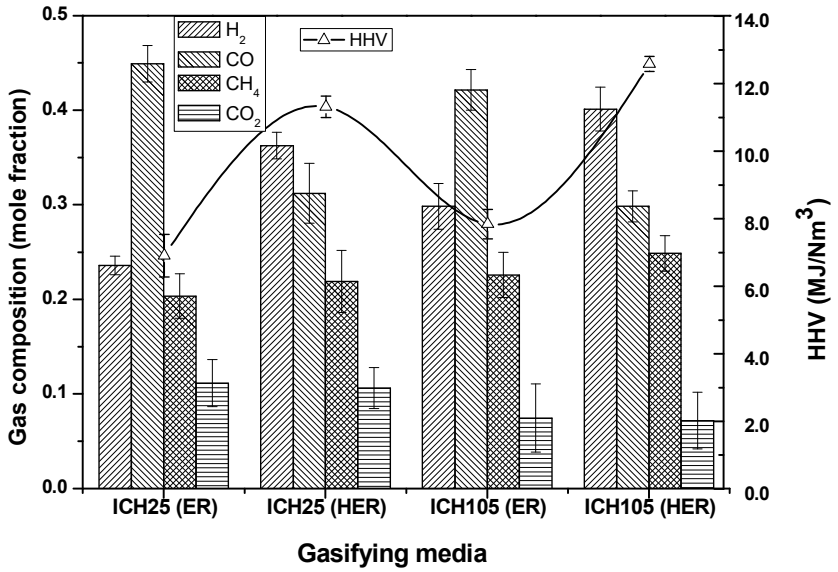

Figure 4.18 Gas composition and HHV with air and humidified air for CO_2 addition for fixed bed gasification

4.4. Gasifier performance for fixed bed gasification of UCH and ICH

The gasifier performance was evaluated initially for UCH at all gasifying conditions which were summarised in Table 4.4. Total gas yield (Y), carbon conversion (η_c) and cold gas efficiency (η) of gasification were calculated with the help of equations 3.1, 3.2 and 3.3. Furthermore, gasification performance of both UCH and ICH25 at optimum condition of gasification parameters (for air at 800 $^{\circ}$C and humidified air as the

gasifying medium at 850 °C) were summarised in Table 4.5 and 4.6. It was seen from Table 4.4 that, carbon conversion was highest 77.53 % at ER 0.4 for UCH and it was comparable at ER 0.3. Furthermore, for ICH25 carbon conversion was also maximum of 86.74 % at ER 0.4. It was due to the partial combustion which produced more CO_2 instead of H_2. Gas yield was also increased with the increase of ER and HER. However, cold gas efficiency was found highest 68.69 % for UCH and 77.11 % for ICH25 in humidified air gasification medium with HER 0.2 and 0.3 respectively. Furthermore, gasifier performances of UCH and ICH25 with air and humidified air as gasifying medium have been given in Table 4.5 and Table 4.6. It was found that at lower ER, cold gas efficiency and carbon conversion was high under humidified air gasification with respect to air gasification. Whereas, when the ER was increased to 0.4, the carbon conversion increased because of combustion instead of gasification.

Table 4.4 Gas yield, carbon conversion and cold gas efficiency of UCH at different experimental operating conditions

Gasifying temperature (°C)	Inlet air			UCH feed	Produced fuel gas		
	ER	Average temperature (°C)	Humidity (%)	Average particle size (mm)	Gas Yield (Nm^3/kg)	Carbon conversion (%)	Cold gas efficiency (%)
700	0.1	33	29	0.72	0.68	14.67	13.06
750	0.1	35	28	0.72	0.69	14.77	12.27
800	0.1	32	30	0.72	0.76	19.33	14.94
850	0.1	35	31	0.72	0.78	22.18	16.65
800	0.2	35	28	0.72	1.61	49.41	36.31
800	0.3	37	27	0.72	2.36	76.63	53.62
800	0.4	35	28	0.72	2.89	77.53	46.05
800	0.1	50	55	0.72	0.78	21.70	19.01

800	0.1	50	75	0.72	0.87	30.96	26.86
800	0.1	50	95	0.72	1.00	42.56	37.85
800	0.1	50	95	0.25	0.99	41.86	38.16
800	0.1	50	95	2	1.00	42.84	37.39
800	0.1	50	95	3	0.97	42.38	35.74
700	0.1	50	95	0.72	0.73	20.77	17.57
750	0.1	50	95	0.72	0.86	32.74	27.22
850	0.1	50	95	0.72	1.30	63.85	55.84

Humidity ratios at saturation (kg H_2O vapour/kg dry air) at 30, 35, and 50 ℃ are 0.027, 0.037 and 0.087

Table 4.5 Gasifier performances for UCH and ICH25 with air as gasifying medium

	Gas yield (Y) (Nm^3/h/kg biomass)		C conversion (η_c) (%)		Cold gas efficiency (η) (%)	
ER	UCH	ICH25	UCH	ICH25	UCH	ICH25
0.1	0.76	0.83	19.33	23.91	14.93	24.23
0.2	1.61	1.71	49.41	46.26	36.30	46.49
0.3	2.36	2.64	76.63	81.35	53.62	66.32
0.4	2.89	3.17	77.52	86.75	46.05	59.53

Table 4.6 Gasifier performances for UCH and ICH25 with humidified air as gasifying medium

	Gas yield (Y) (Nm^3/h/kg biomass)		C conversion (η_c) (%)		Cold gas efficiency (η) (%)	
HER	UCH	ICH25	UCH	ICH25	UCH	ICH25
0.1	1.30	1.03	63.84	26.12	55.84	38.34
0.2	1.96	2.03	78.92	62.28	68.69	74.83
0.3	2.39	2.67	70.16	78.37	60.54	77.11
0.4	2.88	3.13	67.64	80.84	57.57	60.21

4.5. Fuel gas composition on fluidized bed gasification

In this section optimum conditions of previous conditions of previous findings were been taken as reference to start the investigation in fluidized bed gasification. Thus, UCH and ICH105 were taken as raw materials for gasification in fluidized bed operation. Furthermore, several experiments were performed to optimise ER/HER, temperature, and CO_2 air ratios to maximize the fuel gas composition in the produced fuel gas.

4.5.1. Comparison between UCH and ICH via humidified air gasification

As per previous findings, the H_2 content in the fuel gas was more for humidified air in fixed bed gasification compared to air as gasifying medium. So, gasification of UCH and TCH were performed in bubbling fluidized bed reactor at HER of 0.1 and temperature 850 ℃. The results were shown in Figure 4.19. Concentration of C_nH_m was in trace amount and assumed to be neglected. The mole fraction of H_2, CO, CH_4, and CO_2 in fuel gas for UCH gasification were found to be 0.27, 0.32, 0.34 and 0.07, respectively, whereas, in the gasification of ICH105 the H_2 content was increased to 0.56 mole fraction. However, concentration of CH_4 was decreased in gasification of ICH105 giving rise to more H_2 content in fuel gas. And because of this HHV was found to be decreased from 12.31 MJ/Nm^3 for UCH to 5.25 MJ/Nm^3 for ICH105. It was due to the fact that HHV of CH_4 per meter cube basis is approximately 3 fold larger than H_2. Furthermore, concentration of CO_2 was also decreased in ICH105 gasification. The H_2 concentration was 0.40 mole fraction in fixed bed gasification of ICH105 (Figure 4.18). The high amount of H_2 generation in the bubbling fluidized bed of ICH105 was due to the fact that fluidized bed provided more surface area of biomass particles exposed to the gasifying medium and silica sand present as the bed naturally endowed with uniform

temperature distribution. The main secondary reactions are shown by Equations 1.4, 1.5, 1.6 and 1.7 [Mohammed et al., 2011] as given below:

$$Tar + H_2O(g) \rightarrow CO + H_2O + CH_4 + H_2 + C_nH_m \quad (1.6)$$

$$C_nH_m + nH_2O \rightarrow nCO + [n + \left(\frac{m}{2}\right)H_2] \quad (1.7)$$

It could also be inferred that the catalytic activity of impregnation of Na and Ca, etc. assuage the water gas shift reaction (Equation 1.1), methane steam reforming (Equation 1.2), tar steam reforming reaction (Equation 1.6) and, C_nH_m steam reforming (Equation 1.7) and thereby increasing the concentration of H_2 in fuel gas.

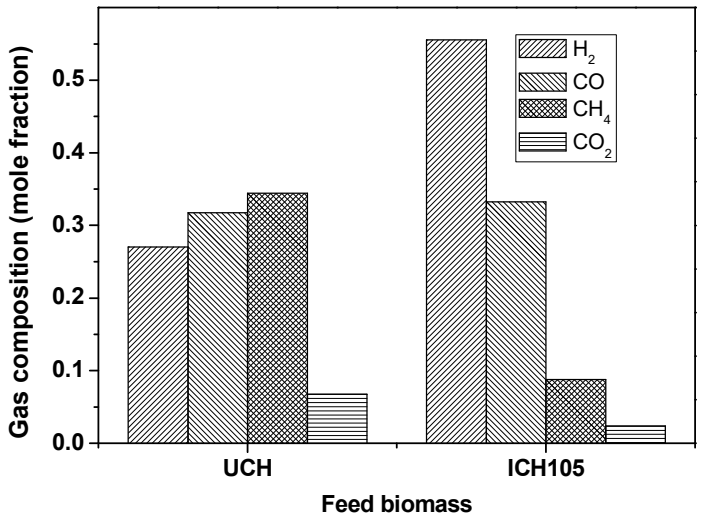

Figure 4.19 Fuel gas compositions produced in fluidized bed gasification of UCH and ICH105

4.5.2. Influence of gasification temperature with HER

Since, high amount of H_2 is required in several synthesis processes and H_2 is considered to be a green fuel, thus, more focus has to be given on the high composition of H_2 in the fuel gas. In addition, temperature is an important and crucial operating parameter for the performance of gasification process. So, gasification was performed with HER of 0.1 and gasification temperature from 750 to 900 ℃ with increment of 50 ℃. Analysis of fuel gas was shown in Figure 4.20 for ICH105. Initially at temperature 750 ℃, H_2 mole fraction was most minimal (0.20 mole fraction) and it was increased with the increase of gasification temperature reaching to maximum of 0.56 mole fractions at 850 ℃. However, its concentration was comparably same at 900 ℃. Furthermore, CO slightly increased from 750 to 800 ℃, then decreased further in the fuel gas. Also, CH_4 concentration was decreased progressively and reached from 0.23 mole fractions to 0.08. Since, formation of CH_4 requires energy supply of 74.8 kJ as laid down in Equation (4.5). So, it can be inferred that lower temperature favours CH_4 formation.

$$C + 2H_2 \rightarrow CH_4 \qquad \Delta H = +74.8\ kJ/\text{mole} \tag{4.5}$$

CO_2 was also followed the same trend as CH_4. The same trends were also reported by other researchers (Zang et al., 2013; Dogru et al., 2002; xiao et al., 2006). Moreover, it was observed that there was not any major change between temperature 850 and 900 ℃. So to save energy, 850 ℃ can be taken as optimum gasification temperature considering maximum H_2 production for the particular set of bubbling fluidized bed gasification setup. However, HHV was decreased drastically with increasing gasification temperature and reached from 7.78 MJ/Nm^3 at 750 ℃ to 5.31 MJ/Nm^3 at 900 ℃

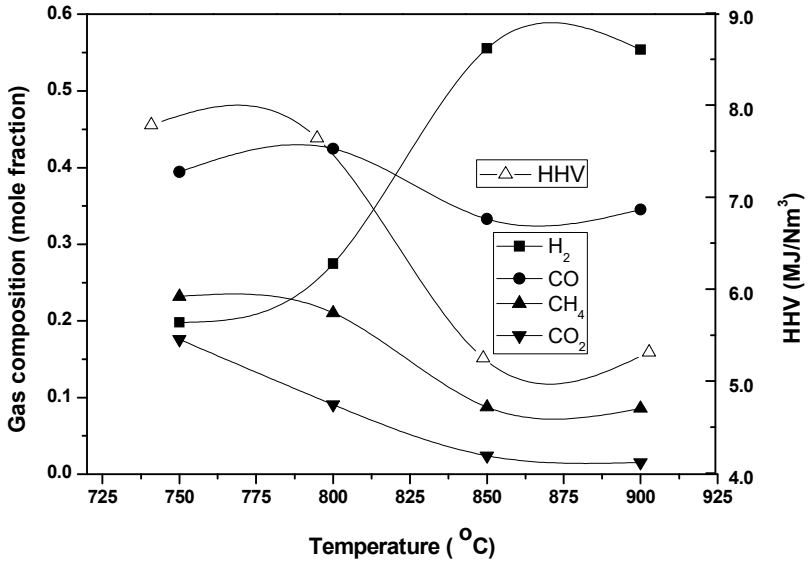

Figure 4.20 Influence of temperature on fuel composition and HHV for fluidized bed gasification

4.5.3. Effect of HER on fuel gas composition

Further experiments were performed to investigate the influence of HER on ICH105 at 850 ℃ and the results were shown in Figure 4.21. It was observed that increasing of HER continuously decreased the H_2 concentration ranging from 0.56 to 0.47 mole fraction. However, CO_2 concentration was observed slightly increasing with the increase of HER due to increase of O_2 in the gasifier. HHV was found highest at HER of 0.2, i.e. 5.43 MJ/Nm^3, it was due to slight increase of CH_4 concentration. Moreover, the mole fraction of CO_2 was increased from 0.02 mole fraction to 0.08. It could be surmised that because of high concentration of O_2, more samples were favouring combustion giving CO_2 in products. The trends were same for UCH and ICH25 for both gasifying medium air and humidified air.

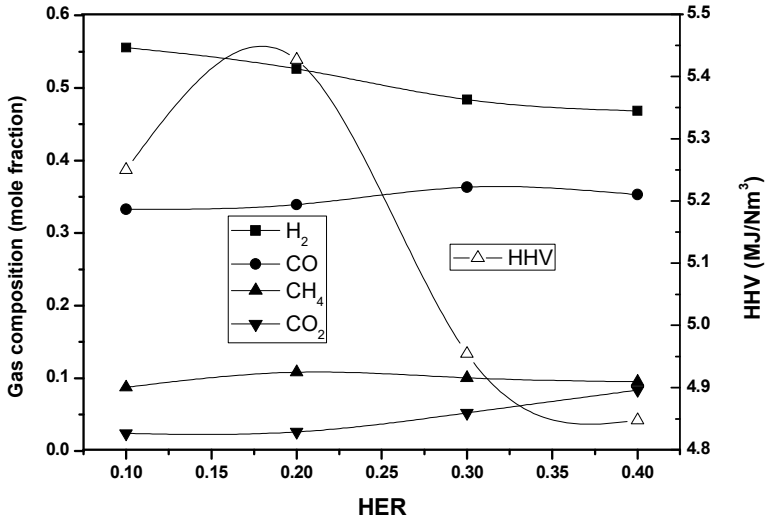

Figure 4.21 Influence of HER on fuel gas composition and HHV for fluidized bed gasification

4.5.4. Synergetic effect of humidified air and CO_2 as gasifying medium

To increase the HHV and maintain the balance between H_2 and CO concentrations in the fuel gas for synthesis purpose, a set of experiments was performed by adding CO_2 gas at different ratios with humidified air as gasifying medium. Flow rate of humidified air was kept constant with HER of 0.1 and addition of CO_2 was done to get the humidified air to CO_2 ratios of 1:1/4, 1:1/3, 1:1/2 and 1:1 by volume. The results were shown in Figure 4.22. Addition of CO_2 increased the composition of CO in the produced fuel gas; however, after increasing CO_2 addition more than 1:½ ratio, CO_2 in fuel gas was increased. There were slight variations (approximately 0.55 to 0.53 mole fraction) in H_2 composition in the fuel gas when CO_2 addition was increased from ¼ to ½. Furthermore, HHV was found maximum at the ratio of 1:1/3 and CO_2 was also considerably low. Therefore, the ratio 1:1/3 of humidified air to CO_2 can be taken as optimum ratio. The additional reaction involved in the CO_2 gasification is Boudouard

reaction (Equation 4.4) which gives rise of CO in the fuel gas by utilizing CO_2 from gasifying medium. Also, according to Equation 1.3 (Mohammed et al., 2011), CH_4 reacts with CO_2 to hasten the formation of both CO and H_2 in the fuel gas. Furthermore, percentage yield of product distribution at optimum condition was investigated and presented in Figure 4.23. The fuel gas, fuel oil and solid residue production after gasification were found to be 87.02, 6.77 and 6.21 %, respectively. Solid residue was near to ash % as shown in Table 4.1.

$$CH_4 + CO_2 \rightarrow 2CO + 2H_2 \quad (1.3)$$

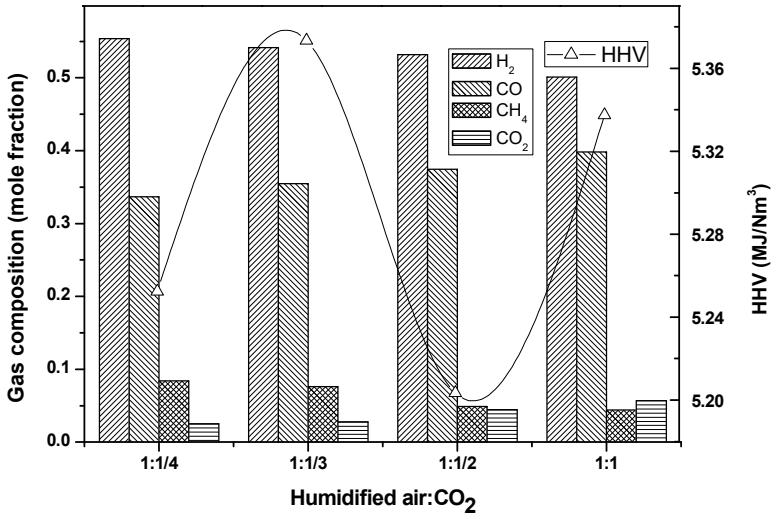

Figure 4.22 Effect of CO_2 addition on fuel gas composition and HHV for fluidized bed gasification

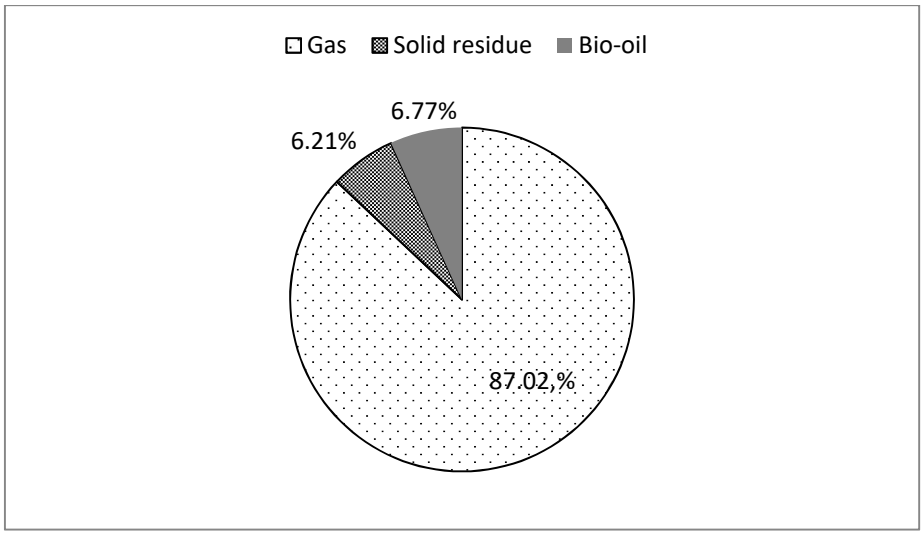

Figure 4.23 Percentage of products after fluidized bed gasification

4.6. Optimization of fuel gas production on fluidized bed gasification using RSM

Fluidized bed provides uniform heating of materials throughout the effective zone of gasifier, in addition it also provides proper contact between solid surface of feedstock and the gasifying medium as gasifying agent. The tar generation is suppressed in fluidized bed gasification because of the uniform heating and proper contact of oxidising agent. And thus high amount of carbon conversion is achieved. Therefore, optimization of process parameters was needed to be done on fluidized bed gasification column. Furthermore, response surface methodology (RSM) is a regression method for finding out the relationship between the independent variable and its response during optimization which uses a collection of mathematical and statistical techniques available in it.

4.6.1. Optimization process parameters

Design Expert software was used in the present study for the optimization of process parameters, and Box-Behnken design (BBD) of RSM was used for the study. BBD method is more efficient than the other methods because of its property for the determination of the response function after very few combinations of variables (Kapur et al., 2016; Ferreira et al., 2007).

The series of experiments were designed and conducted for fluidized bed under humidified air gasifying medium to study the effect of HER, humidified air to CO_2 ratio, and temperature. HER was varied from 0.1 to 0.4. Humidified air to CO_2 ratio was varied from 1 to 2.5 by varying CO_2 and keeping the flow rate of humidified air fixed to maintain desired equivalence ratio. Also, the gasification was performed at three different temperatures, i.e. 800, 850 and 900 ℃. With these experimental parameters, the system was assessed using design expert statistical tool with Box-Behenken design based on the response surface methodology (RSM) for fuel gas composition and HHV of fuel gas. All the process parameters were utilized up to 3 levels 3 factors to compute the quadratic model with 5 centre points. High (+1), centre (0) and, low (-1) are the three factors in BBD. The number of experiments in BBD is given by $N = k^2 + k + r$, where k is the factor number and r is the repeated no of the centre point. Total 17 experimental runs with 12 unique and 5 centre point runs were categorized to assess the effect of process variables on fuel gas composition and HHV of fuel gas.

Furthermore, coefficient of determination (R^2) and three-dimensional plots were evaluated using analysis of variance (ANOVA). The P and F values were also obtained from ANOVA, where P-value indicates whether F-value is large enough to assure statistical significance and F values indicates that the variation in the response can be

illustrated by the regression equation. P-values lower than 0.05 deliver strong evidence that the given model is statistically significant (Dhanavath et al., 2017). Whereas, p-value greater than 0.05 is supposed to be insignificant.

4.6.2. Response with parameters

Responses of all 17 experimental runs including 5 centre points have been tabulated in Table 4.7. The individual composition of components (H_2, CO, CH_4, and CO_2) in fuel gas with the variation of HER and humidified air to CO_2 ratio have been shown in Figures 4.24 to 4.27. The ranges of composition were found as 0.33-0.55 for H_2, 0.29-0.43 for CO, 0.07-0.25 for CH_4, and 0.02 to 0.07 for CO_2 in mole fraction. In addition, HHV was varied from minimum 4.25 to maximum 5.73 MJ/Nm^3 during the study. The highest and lowest compositions of H_2 were found at gasification temperature 850 and 800 °C, HER 0.1 and 0.4, humidified air to CO_2 ratio 1:1/4 and 1:1/2.5, and the values were 0.55 and 0.33 mole fraction respectively. Quadratic model was suggested by ANOVA for each component for maximizing the adjusted R. ANOVA also showed the terms were significant and the model was aliased. All the models for each variable were significant with the p-value less than 0.0001. However, for the significant terms p-value of the regression model considered to be less than 0.05. The p-value less than 0.05 was found to provide assurance of 95%. The R^2 and adjusted R^2 were used to predict whether the models are over fitting or having random noises. The value of R^2 increases with more independent variable, whereas predicted R^2 values increases with the elimination of insignificant variables. Here, the adjusted R^2 of the regression models were shown close to 85%, thus, the predicted models can be considered as satisfactory for the fluidized bed gasification in the column in which the experiments were performed. In addition, since, the difference between the adjusted R^2 and the predicted R^2 are less than 10% for the composition of H_2 component this model can be used to

pilot the design space. However, since, the regression model for CO, CH_4, and CO_2 are 19, 16, and 14 %, respectively, therefore, these models can also be used for the predication of H_2, CO, CH_4, and CO_2 compositions in fuel gas by data correlations. Furthermore, data correlations for the prediction of composition of H_2, CO, CH_4, and CO_2 have been given in equations (4.6) to (4.9), respectively.

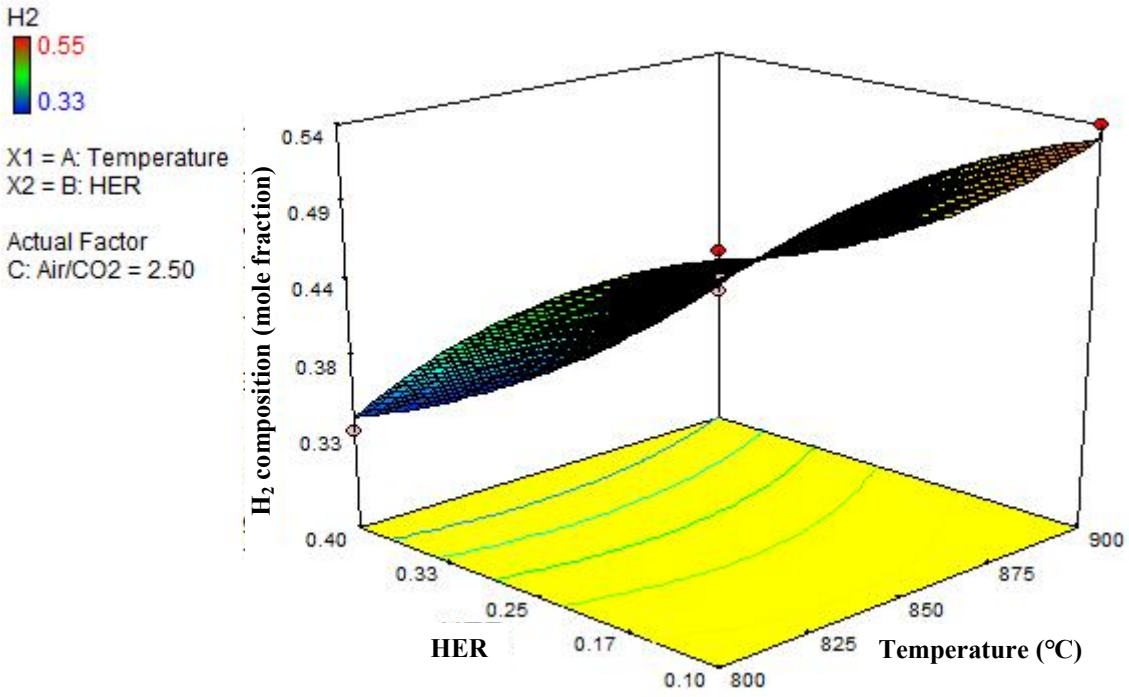

Figure 4.24 H_2 concentrations with temperature and HER for fluidized bed gasification

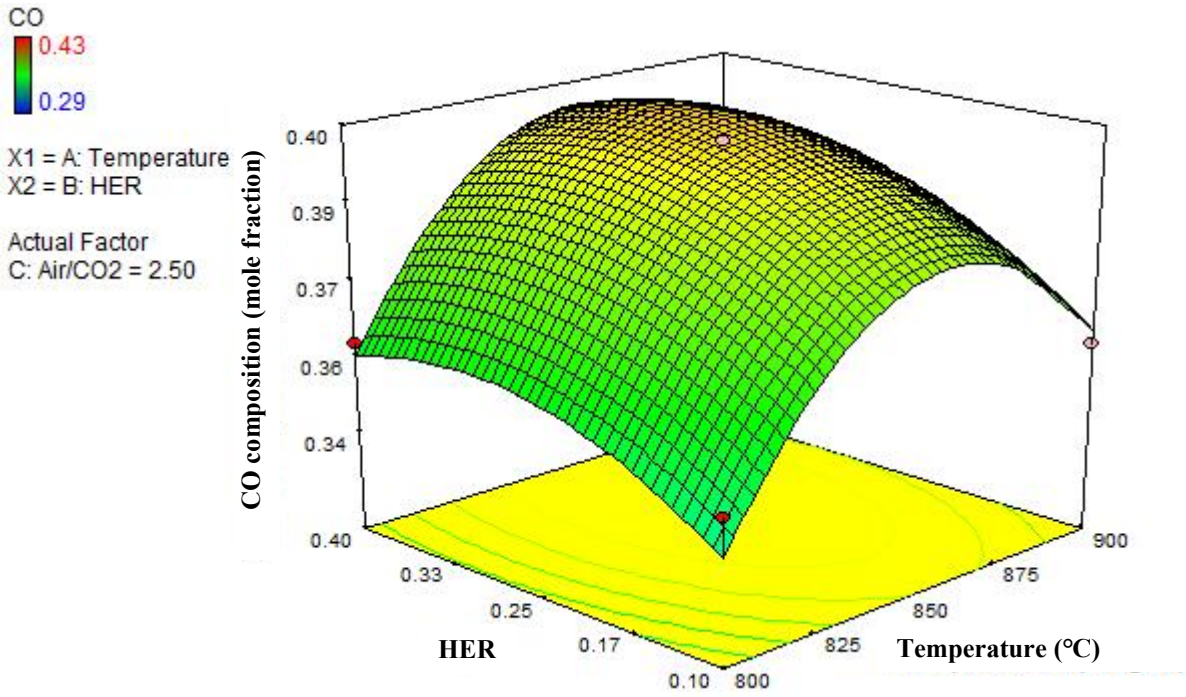

Figure 4.25 CO concentrations with temperature and HER for fluidized bed gasification

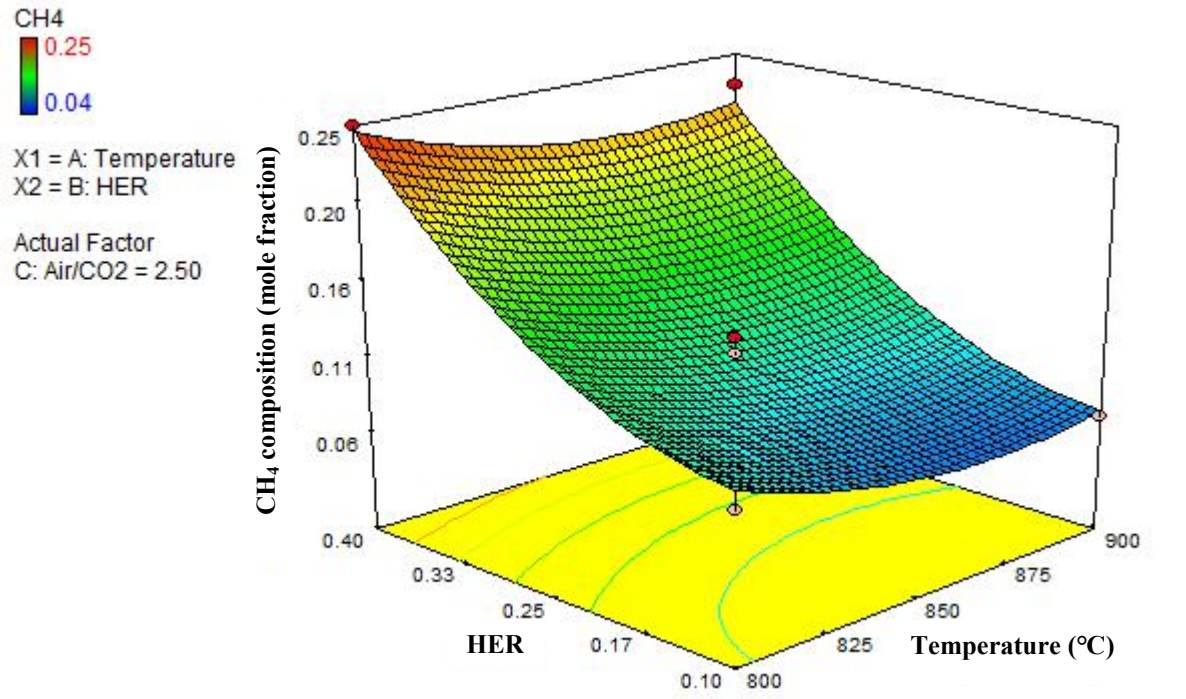

Figure 4.26 CH_4 concentrations with temperature and HER for fluidized bed gasification

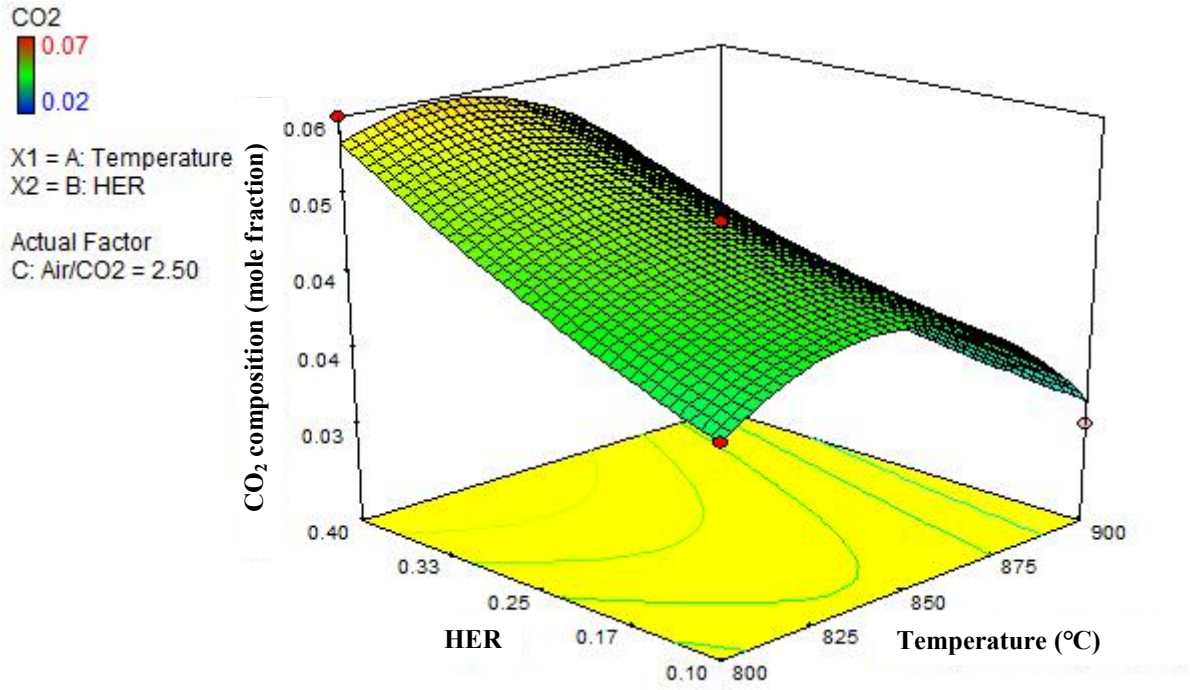

Figure 4.27 CO_2 concentrations with temperature and HER for fluidized bed gasification

Table 4.7 Experimental factors and their responses

Run	Factors			Responses (mole fraction)				
	Temperature (°C)	HER	Humidified air:CO_2	H_2	CO	CH_4	CO_2	HHV (MJ/Nm^3)
1	800	0.4	2.5	0.3263	0.3587	0.2547	0.0603	5.38
2	900	0.4	2.5	0.3573	0.3727	0.2275	0.0425	5.41
3	850	0.25	2.5	0.4429	0.3981	0.1122	0.0468	5.21
4	900	0.1	2.5	0.5357	0.3619	0.0706	0.0318	5.31
5	850	0.4	4	0.3742	0.3538	0.2308	0.0412	4.25
6	850	0.1	1	0.5009	0.3980	0.0441	0.0570	5.40
7	850	0.4	1	0.3652	0.4327	0.1524	0.0697	5.34
8	900	0.25	1	0.4718	0.3983	0.0772	0.0527	5.52
9	850	0.25	2.5	0.4411	0.3961	0.1167	0.0461	5.73

10	850	0.1	4	0.5537	0.3367	0.0842	0.0254	5.26
11	850	0.25	2.5	0.4431	0.3973	0.1139	0.0457	4.93
12	800	0.25	1	0.4723	0.3994	0.0658	0.0625	5.32
13	800	0.1	2.5	0.5177	0.3472	0.0928	0.0423	5.58
14	800	0.25	4	0.4918	0.2905	0.1894	0.0283	4.61
15	900	0.25	4	0.5187	0.3485	0.1084	0.0244	4.61
16	850	0.25	2.5	0.4417	0.3989	0.1123	0.0471	5.28
17	850	0.25	2.5	0.4438	0.3994	0.1093	0.0475	5.24

Table 4.8 Data of analysis of variance

ANOVA parameters	**H_2**	**CO**	**CH_4**	**CO_2**
Model suggested	Quadratic	Quadratic	Quadratic	Quadratic
F value	586.53	303.19, 99.34	381.26, 86.52	445.50, 96.97
p-value	<0.0001	<0.0001	<0.0001	<0.0001
Significant terms	B	C, A^2	B, C	C, B
R-squared	0.9936	0.9861	0.9879	0.9889
Adj R-squared	0.9854	0.9683	0.9723	0.9746
Pred R-squared	0.8991	0.7836	0.8130	0.8339
Coefficient of varience (%)	1.76	1.62	8.17	4.53

Data correlations

$$H_2 = (44.25+0.94*A-8.56 * B+1.60 * C+0.32 *A* B+0.68 *A* C-1.09 *B*C+1.59*A^2-2.42 * B^2+3.02*C^2)/100 \quad (4.6)$$

$$CO = (39.80+1.07*A+0.93*B-3.74*C-0.018*A*B+1.48*A*C-0.44*B*C-2.95*A^2-0.84*B^2-0.93*C^2)/100 \quad (4.7)$$

$$CH_4= (11.29-1.49*A+7.17*B+3.42*C-0.13*A*B-2.31*A*C+0.96*B*C+1.54*A^2+3.31*B^2-1.81*C^2)/100 \quad (4.8)$$

$$CO_2= (4.66-0.53*A+0.72*B-1.53*C-0.18*A*B+0.15*A*C+0.078*B*C-0.44*A^2+0.20*B^2-0.028*C^2)/100 \quad (4.9)$$

Where, composition of each component is in mole fraction, A is temperature in ℃, B is HER, and C is Humidified air to CO_2 ratio.

4.6.3. Optimized response

Keeping the temperature and HER in range, the process was optimized for maximum composition of H_2 and CO and minimum composition of CH_4 and CO. By giving 5* importance to maximizing of H_2 and CO and minimizing of CO_2 the ANOVA has generated total 8 solutions with the highest desirability of 0.837. The optimized temperature, HER and humidified air to CO_2 ratio were predicted as 887.56 ℃, 0.13, and 3.74, respectively. The predicted compositions of H_2, CO, CH_4, and CO_2 was 0.55, 0.35, 0.69 and 0.02 mole fractions, respectively. Furthemore, the experiments was performed at nearest achievable temperature, i.e at 888 ℃ and at suggested HER and humidified air to CO_2 ratio. The experimental value of composition of each component was in agreement of the predicted value with the error of 4.38, 5.29, less than 1, and 22.45 % respectively for H_2, CO, CH_4, and CO_2, which has been also tabulated in Table 4.9.

Table 4.9 Process validation

	Factors			Responses (mole fraction)			
	Temperature (°C)	HER	Humidified air:CO_2	H_2	CO	CH_4	CO_2
Predicted	887.56	0.13	3.74	0.5543	0.3514	0.0698	0.0245
Experimental	888	0.13	3.74	0.53	0.37	0.07	0.03
Error (%)	-	-	-	4.38	5.29	<1	22.45

4.7. Characteristics of by-products

4.7.1. Fuel oil

4.7.1.1. Fourier-transform infrared spectroscopy

Fourier-transform infrared spectroscopy (FTIR) is a technique used to identify various functional groups of the component present in the fuel oil. In this study fuel oil collected from UCH at optimum condition (humidified air gasification temperature of 850 °C with humidity 95%) was investigated by FTIR spectra in the wavelength range of 400 to 4000 cm^{-1} (ALPHA BRUKER Eco-ATR) in attenuated total reflection (ATR) mode. FTIR spectra of fuel oil were shown in Figure 4.28 and the functional groups with classification of compounds were listed in Table 4.10. The strong absorption was observed at absorption peak of 3371 cm^{-1} which was attributed to phenolic OH and COOH groups, and the presence of oxygenated compounds. The presence of alkanes group was indicated by the peak of C-H stretching vibrations between 2800 and 3000 cm^{-1} (peak at 2908 cm^{-1}) and by C-H deformation vibrations between 1350 and 1475 cm^{-1} (peaks at 1434 cm^{-1}) (Gaurh and Pramanik, 2018). The intense peak 1612 cm^{-1} represented C=C stretching vibrations, which was indicative of alkenes. In addition, the

absorbance peaks at 1730-1150 cm^{-1}, corresponding to the presence of heteroatoms (i.e. N and O) functionality, were also observed, which was consistent with results of the GC-MS analysis presented in Table 4.11. The peaks appeared at wavelength 1434 cm^{-1} and 1250 cm^{-1}, attributable to the aromatic stretching vibrations, indicating the presence of aromatic compounds in fuel oil. The peaks between 1000 and 1200 cm^{-1} were due to the presence of alcohols, phenols, ethers and esters showing the C-O stretching vibrations. The similar result was reported in steam gasification by Wei et al., (2007) and Yang et. al. (2007) also got the same trend.

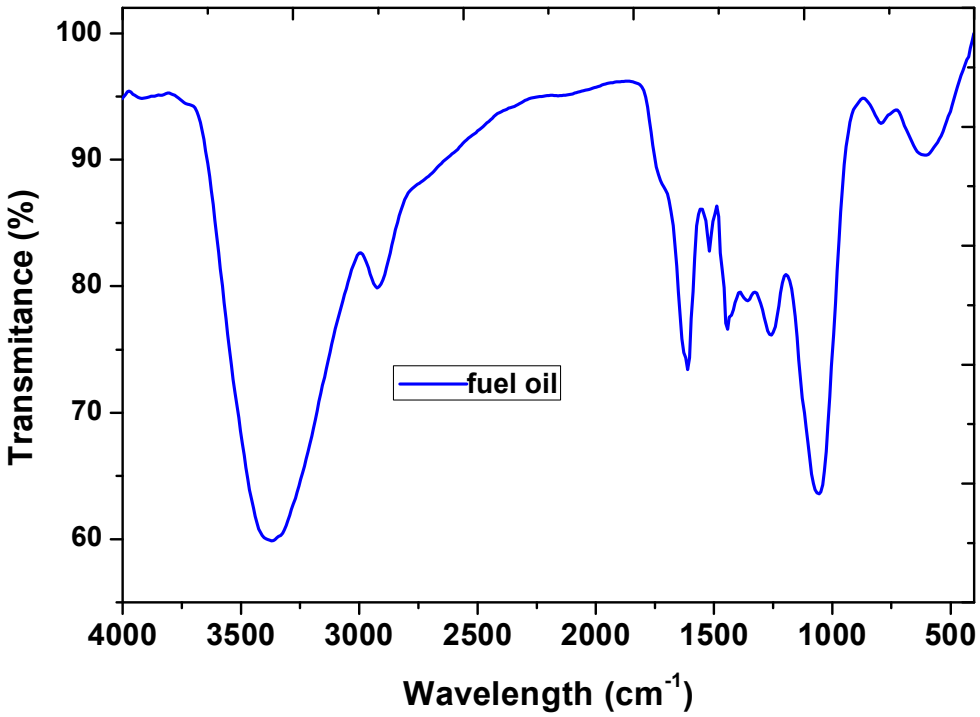

Figure 4.28 FTIR spectra of fuel oil of UCH via humidified air gasification at temperature 850 ℃ and RH 95 %

Table 4.10 FTIR of fuel oil produced from UCH via humidified air gasification at temperature 850 ℃ and RH 95 %

Frequency range, cm^{-1}	Frequency (fuel oil), cm^{-1}	Group	Class of component
3600-3300	3371	O-H stretching	Polymeric O-H
3050-2800	2908	C-H stretching	Alkanes
1570-1680	1612	C=C stretching	Alkenes
1475-1525	1511	C=C ring stretching	Aromatics
1475-1330	1434	C-H deformation	Alkanes
1280-1200	1250	C-H stretching	Aromatics
1000-1200	1050	C-O stretching	Alcohols, esters, ethers
750	750	Adjacent C-H deformation	Aromatics
615	617	Out of plan O-H deformation	Polymeric O-H

4.7.1.2. Gas chromatography mass spectroscopy

Gas chromatography mass spectroscopy (GC-MS) analysis of fuel oil produced from UCH at 850 ℃ and RH 95% was done in order to identify the components present in the produced fuel oil at optimum condition. The number of compounds detected by GC-MS analysis indicating retention time of each component was plotted in Figure 4.29. Furthermore, it was compared with the GC-MS library and the results were tabulated in Table 4.11. It can be seen from table 4.11 that the total 45 components were detected by GC-MS analysis with very complex mixtures of C5 to C24 organic compounds. However, phenol and catechol were present in appreciable amount and few (12) compounds were present between 10 to 1 % of total area, and major (31) compounds were present only in traces. Most abundant products were considered as compounds

with peak areas near or greater than 2% (Ozbay et al., 2008). It was seen that fuel oil was mainly composed of phenols, acid, alkanes, furances, ketones, alcohols and nitrogen-bearing heterocyclic compound, pyridine. The components of the fuel oil were similar to the liquid product studied by other researchers using other biomasses (Chen et al., 2017; Zeng et al., 2017). Oxygen-rich primary tars like acids are mainly formed from the high oxygen content cellulose and hemicellulose degradation at low temperature (Wolfesberger et al., 2009). The area of most abundant compound phenols was 24.29 %. These derivatives of phenolic fragments might be derived from the thermal decomposition of protein present in UCH, which are known as the polyphenolic components in biomass (Chen et al., 2017). Moreover, at moderate temperature around 850 °C, more secondary tars such as phenols were produced by decarboxylation, decarbonylation (Cypres, 1987) and dehydrogenation after Diels-Alder reactions (Morf et al., 2002) of primary tar. The 1,2-benzenediol, 4-methyl- (11.21 area %), 2,6-dimethoxy- (5.87 area %), pyrazine, 2,6-dimethyl- (1.95 area %), 3-Methylcyclopentane-1,2-dione (1.84 area %) appear as main compounds in the fuel oil of humidified air gasification as indicated in Table 4.11. The nitrogen-containing heterocyclic compound in fuel oil, such as pyridines, was assumed to be derived from protein degradation (Zhou et al., 2010). Tar may be formed at lower amount below the GC/MS detection limit. Phenol, alkane, alkynes, ketones were also confirmed with FTIR of fuel oil. This result is consistent with the FTIR result of fuel oil.

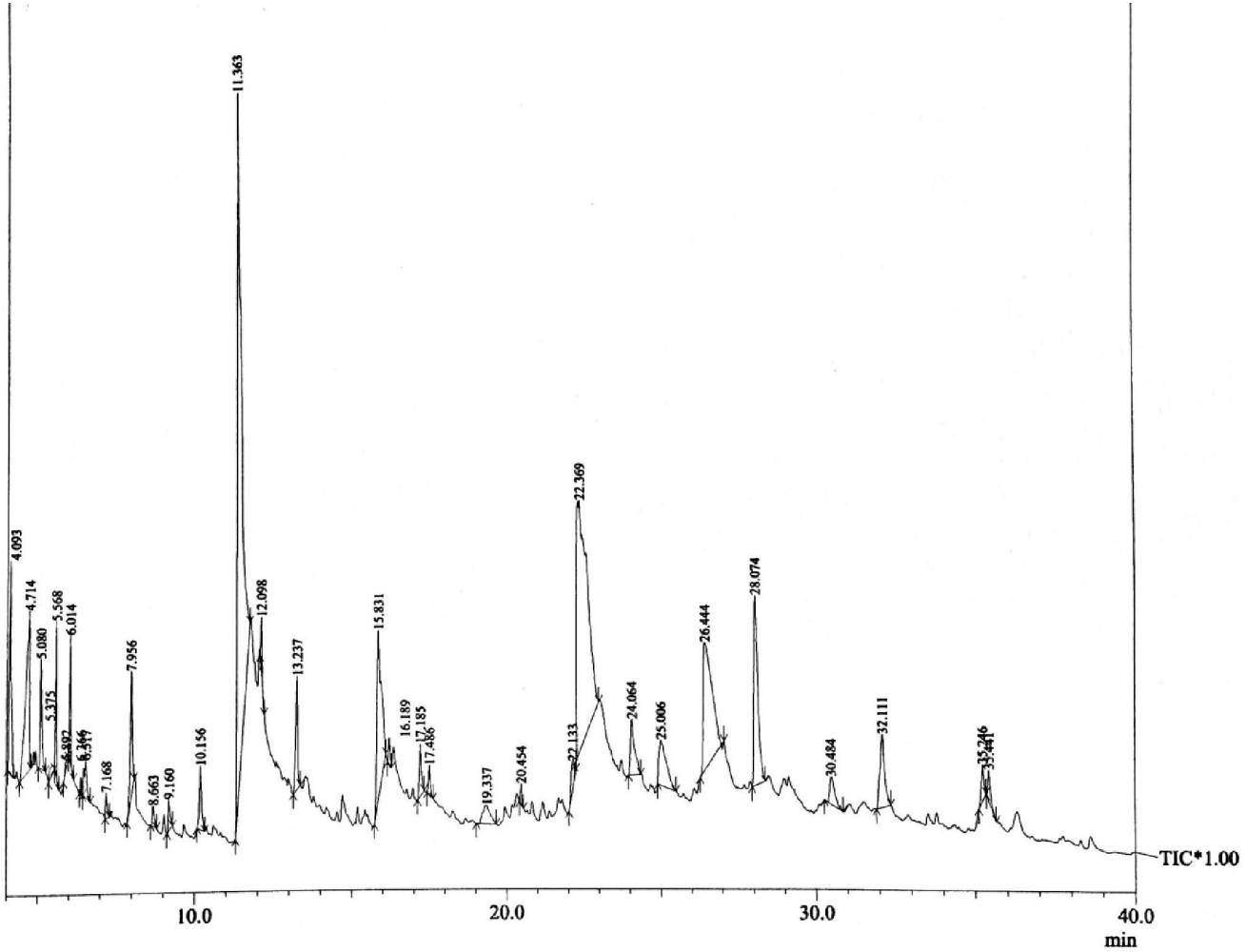

Figure 4.29 GC-MS spectrum of fuel oil of UCH via humidified air gasification at temperature 850 ℃ and RH 95 %

Table 4.11 GC-MS of fuel oil produced from UCH via humidified air gasification at temperature 850 ℃ and RH 95 %

Sl. no.	Retention Time	Area %	Name of compound	Molecular Formulae
1	4.093	2.92	1,3-Dioxolane, 2,2,4,5-tetramethyl-, cis-	$C_7H_{14}O_2$
2	4.714	4.78	1-Propanol, 2,2-dimethyl-, acetate	$C_7H_{14}O_2$
3	5.08	1.28	Pyridine, 2-methyl-	C_6H_7N
4	5.375	0.3	sobutyldimethylcarbinol	$C_7H_{16}O$
5	5.568	1.18	2-Hydroxy-2-methyl-4-pentanone (diacetone)	$C_6H_{12}O_2$
6	5.892	0.15	2-Furanmethanol	$C_5H_6O_2$
7	6.014	1.23	2-Furanmethanol	$C_5H_6O_2$
8	6.366	0.13	2-(Acetyloxy)ethyl acetate	$C_6H_{10}O_4$
9	6.517	0.79	Pyridine, 3-methyl-	C_6H_7N
10	7.168	0.29	2,6-Lutidine	C_7H_9N
11	7.956	1.95	Pyrazine, 2,6-dimethyl-	$C_6H_8N_2$
12	8.663	0.3	8-Azabicyclo[3.2.1]oct-6-en-3-one, 8-methyl-	$C_8H_{11}NO$
13	9.16	0.43	Pyridine, 2,4-dimethyl-	C_7H_9N
14	10.156	1.05	2-Cyclopenten-1-one, 3-methyl-	C_6H_8O
15	11.363	24.29	Phenol	C_6H_6O
16	12.098	0.54	Pyrazine, trimethyl-	$C_7H_{10}N_2$
17	13.237	1.84	3-Methylcyclopentane-1,2-dione	$C_6H_8O_2$
18	15.831	5.82	Phenol, 4-methyl-	C_7H_8O
19	16.189	0.33	2,5-Pyrrolidinedione, 1-methyl-	$C_5H_7NO_2$
20	17.185	0.88	4H-pyran-4-one, 3-hydroxy-2-methyl-	$C_6H_6O_3$
21	17.486	0.38	2-Cyclopenten-1-one, 3-ethyl-2-hydroxy-	$C_7H_{10}O_2$
22	19.337	1.04	2,5-Pyrrolidinedione	$C_4H_5NO_2$
23	20.454	0.23	2,3,5-Trimethyl-6-propylpyrazine	$C_{10}H_{16}N_2$
24	22.133	0.79	1,4:3,6-Dianhydro-.alpha.-d-glucopyranose	$C_6H_8O_4$
25	22.369	21.24	Catechol	$C_6H_6O_2$
26	24.064	1.75	1,2-Benzenediol, 3-methoxy-	$C_7H_8O_3$
27	25.006	2.57	1,2-Benzenediol, 3-methyl-	$C_7H_8O_2$

28	26.444	8.64	1,2-Benzenediol, 4-methyl-	$C_7H_8O_2$
29	28.074	5.87	Phenol, 2,6-dimethoxy-	$C_8H_{10}O_3$
30	30.484	1.04	4-Ethylcatechol	$C_8H_{10}O_2$
31	32.111	2.51	Tri-o-methylpyrogallol	$C_9H_{12}O_3$
32	35.246	0.72	2-Tert-butyl-4-(hydroxtmethyl)-5-formylfuran	$C_{10}H_{14}O_3$
33	35.441	0.53	2-Propanone, 1-(4-hydroxy-3-methoxyphenyl)-	$C_{10}H_{12}O_3$
34	42.617	0.19	Benzene, ethylphenoxy-	$C_{14}H_{14}O$
35	43.459	0.16	2,4-Hexadienedioic acid, 3,4-diethyl-, dimethyl ester, (E,Z)-	$C_{12}H_{18}O_4$
36	44.939	0.16	Benzoic acid, 2-hydroxy-, phenylmethyl ester	$C_{14}H_{12}O_3$
37	45.79	0.14	Dibutyl phthalate	$C_{16}H_{22}O_4$
38	46.89	0.11	Phytol	$C_{20}H_{40}O$
39	46.99	0.1	9,12-Octadecadienoyl chloride, (Z,Z)-	$C_{18}H_{31}ClO$
40	47.077	0.24	Phytol	$C_{20}H_{40}O$
41	48.351	0.19	cis-Methyl 11-eicosenoate	$C_{21}H_{40}O_2$
42	49.085	0.1	Phenol, 2,4-bis(1-phenylethyl)-	$C_{22}H_{22}O$
43	49.177	0.1	Phenol, 2,4-bis(1-phenylethyl)-	$C_{22}H_{22}O$
44	49.52	0.18	Methyl dihydromal valate	$C_{19}H_{36}O_2$
45	49.699	0.54	1,2-Benzenedicarboxylic acid	$C_{24}H_{38}O_4$

Furthermore, GC-MS analysis of fuel oil produced from ICH105 in fluidized bed gasifier at 850^{o}C and HER 0.1 was also performed in order to identify the components present in the produced fuel oil from fluidized bed gasifier. The number of compounds detected by GC-MS analysis indicating retention time of each component was plotted in Figure 4.30 and it has been tabulated in Table 4.12 after comparison with the GC-MS library. It can be seen from Table 4.12 that the total 32 components were detected from GC-MS analysis with very complex mixtures of C5 to C24 organic compounds. However, phenol, catechol, 1,2-benzenediol, 4-methyl- only were present in appreciable amount and few (7) compounds were present between 10 to 1 % of total area and rest compounds were present only in very small amounts. The major abundant products

were considered as compounds with peak areas near or greater than 2% (Chen et al., 2017). Total 45 numbers of components were present in fuel oil from UCH before treatment as shown in Figure 4.29 which was diminished to 32 after impregnation with pulp and paper industry waste water subjected to fluidization during gasification. It could be surmised that the Na and Ca present onto the ICH105 (Table 4.3) acted as efficient catalysis and responsible for breaking down of higher hydrocarbons.

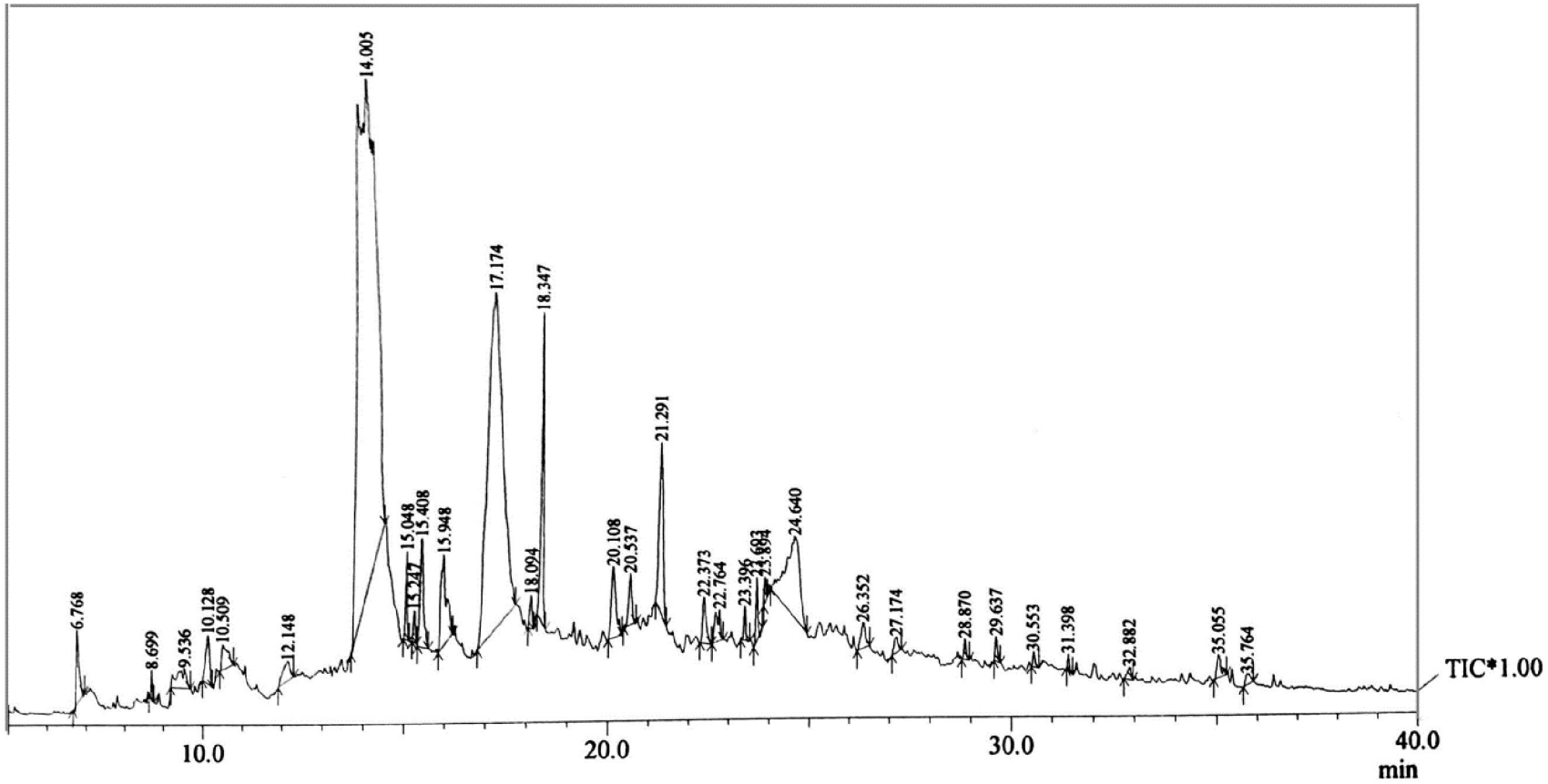

Figure 4.30 GC-MS of bio-oil of ICH105 at HER 0.1 and gasification temperature 850 ℃

Table 4.12 GC-MS of bio oil produced from ICH105 at HER 0.1 and fluidized bed gasification temperature 850 ℃

Peak#	R.Time	Area	Area%	Compound name
1	6.768	2475300	1.01	Phenol
2	8.699	455310	0.19	Octane, 5-ethyl-2-methyl-
3	9.536	2355528	0.96	m-Cresyl butanoate
4	10.128	2342992	0.96	Diazene, bis(1,1-dimethylethyl)-
5	10.509	1904411	0.78	4H-pyran-4-1, 3-hydroxy-2-methyl-
6	12.148	1740631	0.71	2,5-pyrrolidinedione
7	14.005	1.11E+08	45.53	Catechol
8	15.048	1796292	0.73	Benzene, 1,3-bis(1,1-dimethylethyl)-
9	15.247	785238	0.32	Guanosine
10	15.408	4488888	1.83	1,2-Benzenediol, 3-methoxy-
11	15.948	6045350	2.47	Homopyrocatechol
12	17.174	59009978	24.12	1,2-Benzenediol, 4-methyl-
13	18.094	920536	0.38	5-(Hydroxymethyl) dihydro-2(3H)-furanone
14	18.347	8052227	3.29	Phenol, 2,6-dimethoxy-
15	20.108	3860931	1.58	4-Ethylcatechol
16	20.537	2017403	0.82	Ethanone, 1-(3-hydroxyphenyl)-
17	21.291	8532903	3.49	Benzoic acid, 3-hydroxy-, methyl ester
18	22.373	2045435	0.84	Methyl 4-hydroxybenzoate
19	22.764	1854211	0.76	Hexadecane
20	23.396	693961	0.28	2,4-Ditert-butylphenol
21	23.693	1333572	0.54	Benzene, 1,2,3-trimethoxy-5-trimethoxy-5-methyl-
22	23.894	550041	0.22	2-Propanone, 1-(4-hydroxy-3-methoxyphenyl)-
23	24.64	13651551	5.58	.beta.-D-Glucopyranose, 1,6-anhydro-

24	26.352	1398536	0.57	.alpha.-D-Glucopyranose, 4-O-.beta.-D-galactopyranosyl-
25	27.174	780186	0.32	d-Gluco-heptulosan
26	28.87	507458	0.21	Octadecane
27	29.637	657532	0.27	Ethanone, 1-(4-hydroxy-3,5-dimethoxyphenyl)-
28	30.553	379370	0.16	Mandelic acid, 3,4-dimethoxy-, methyl ester
29	31.398	328851	0.13	1-Heptadecene
30	32.882	497154	0.2	Pyrrolo[1,2-a]pyrazine-1,4-dione, hexahydro-3-(2-methylpropyl)-
31	35.055	1181892	0.48	5H,10H-Dipyrrolo[1,2-A:1',2'-D]pyrazine-5,10-dione, octahydro-, (5AS-CIS)
32	35.764	648501	0.27	n-Hexadecanoic acid

4.7.2. Solid residue

Solid product was collected as a leftover residue after gasification process of UCH and ICH. Most important characteristics for solid residue include BET surface area and surface morphology. The reactivity and combustion behaviour of solid residue is strongly affected by surface area (Demiral and Kul, 2014). The BET surface area and total pore volume of UCH solid residue were found to be 173.43 m^2/g and 0.074733 cm^3/g, respectively. Gasification process developed micro and macro pores onto surface of solid residue that increased its porosity. The solid residue of UCH of this study showed high BET surface area as compared to solid residue from other materials in the literature (Gupta et al., 2017; Ie et al., 2012). The SEM images were shown in Figure 4.31a and 4.31b for UCH and Figure 4.32 for ICH25. SEM images of both UCH and ICH25 indicated that there were rough and disorganized structures with negligible pores prior to gasification but solid residue showed surface like honeycomb structure after

gasification. This porous nature of solid residue contributes to increase in the surface area and may be used as adsorbent in adsorption operation (Ie et al., 2012).

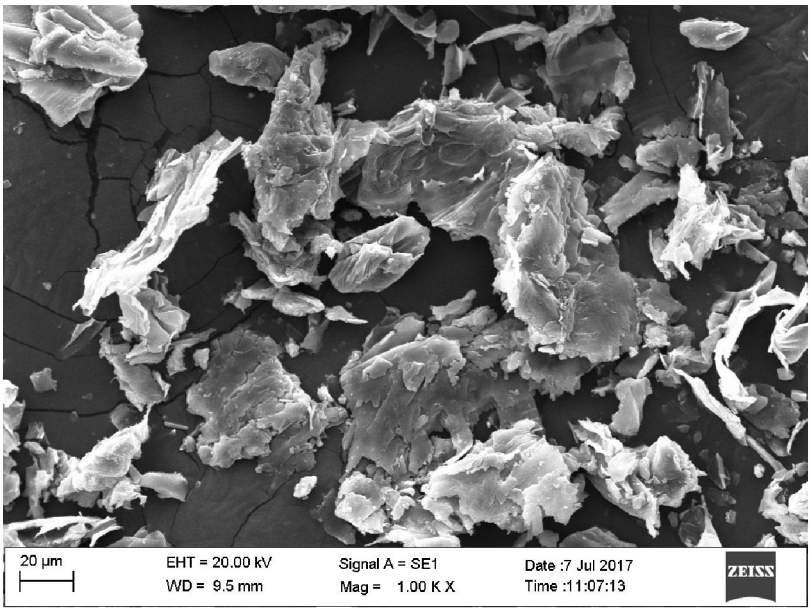

(a)

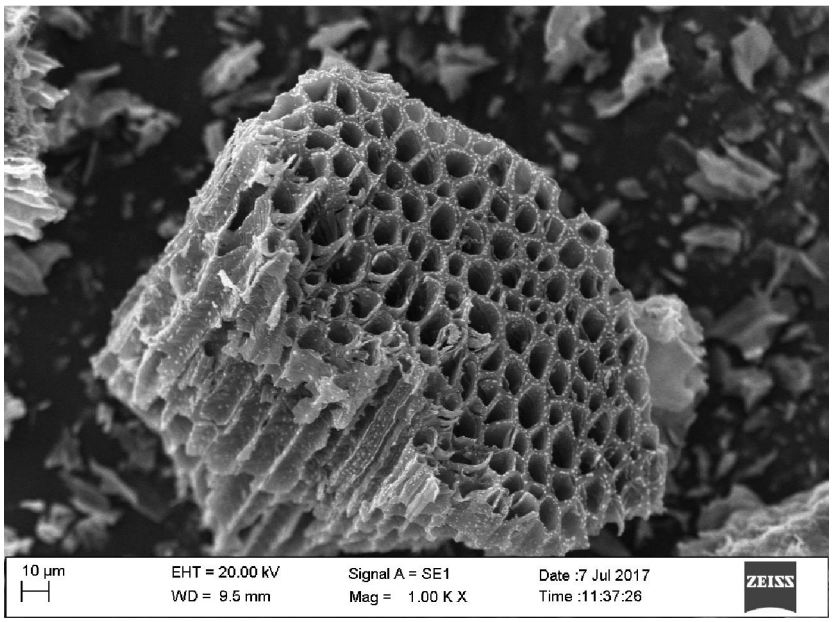

(b)

Figure 4.31 Surface morphology analysis of a) UCH, and b) solid residue of UCH via humidified air gasification at temperature 850 ℃ and RH 95 %

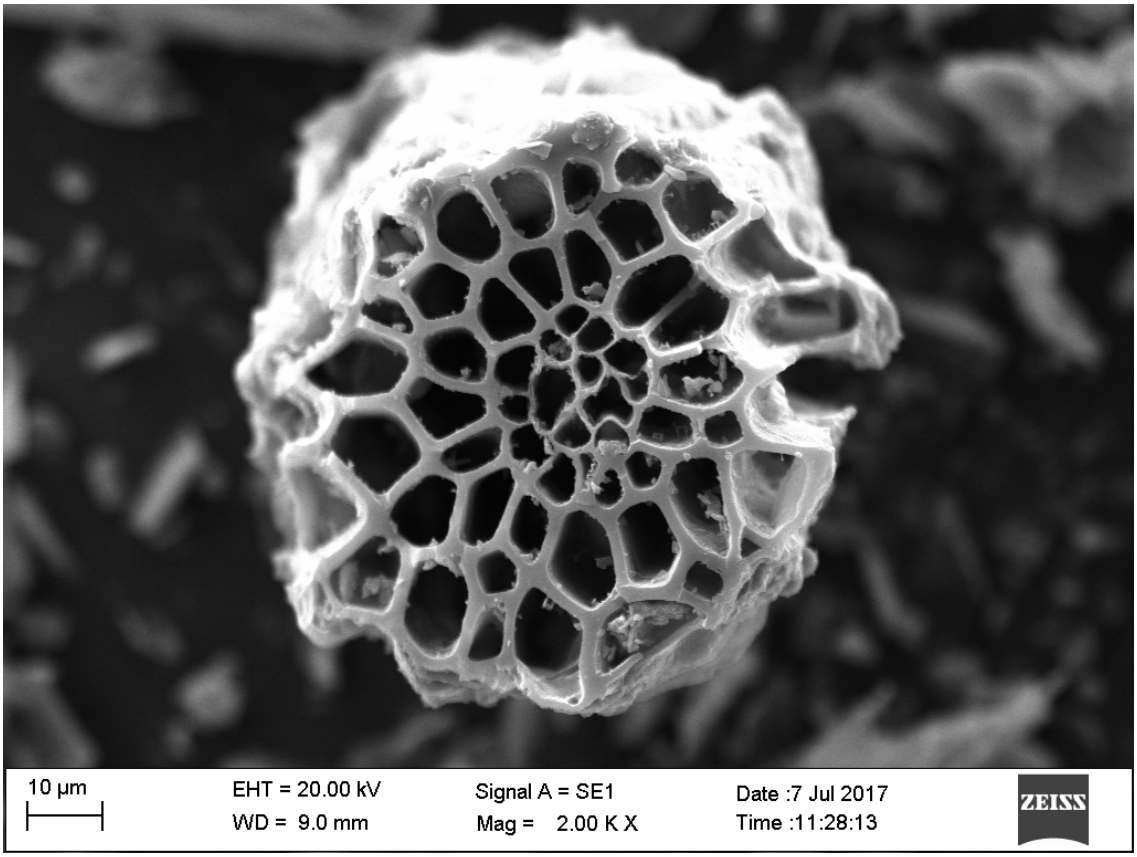

Figure 4.32 Surface morphology of solid residue of ICH25